EE724 HW3

Kartik Chikkanagoudar - 21D170023
Atharv Kulkarni -210070047
Tanveer Molla - 22M1138

Date : 15/02/2004

Ans 7 a)

The poisson equation for a semiconductor is given as

$$\frac{\partial^2 V}{\partial x^2} = -\frac{q\rho}{\varepsilon} \quad \text{where } \rho = N_D + p(x) - N_a - n(x)$$

Now using fermi-dirac statistics we know

$$n = n_i e^{\left(\frac{E_f - E_i}{kT}\right)} \Rightarrow \frac{n}{n_i} = \exp\left(\frac{E_f - E_i}{kT}\right) = \exp(\phi)$$

where $\phi = \frac{E_f - E_i}{kT}$ is a unitless energy.

Similarly since $n \cdot p = n_i^2 \Rightarrow \frac{p}{n_i} = \exp(-\phi)$

$\therefore$ Our poisson equation becomes

$$\frac{\partial^2 V}{\partial x^2} = n_i \frac{-q}{\varepsilon}\left(\frac{N_D - N_A}{n_i} + \frac{p}{n_i} - \frac{n}{n_i}\right)$$

$$\frac{\partial^2 \phi}{\partial x^2} = \frac{-q^2 n_i}{kT\varepsilon_0}\left(\exp(-\phi) - \exp(\phi) + c\right)$$

since $\phi = \frac{E_F - E_i}{kT} = \frac{q(\overbrace{V_F + V}^{\text{constant}})}{kT}$ and $c = \frac{N_D - N_A}{n_i}$

$$\therefore \frac{\partial^2 \phi}{\partial X^2} = -\left(\exp(-\phi) - \exp(\phi) + C\right) \text{ where } \frac{1}{\lambda_D^2} = \frac{q^2 n_i}{KT\varepsilon}$$

here also $X = \frac{x}{\lambda_D} \Rightarrow$ dimension less distance

Now say you know the value of ϕ_{old} at a given time. A small timestep later the new value of ϕ is ϕ_{new} s.t $\phi_{new} - \phi_{old} = \delta$, $\delta \to 0$

$\therefore$ We can say, on linearization $\Rightarrow$

$$\frac{\partial^2 \phi_{new}}{\partial X^2} = -\left(\exp(-(\phi_{old}+\delta)) - \exp(\phi_{old}+\delta) + C\right)$$

$$= -\left(e^{-\phi_{old}} e^{-\delta} - e^{\phi_{old}} e^{\delta} + C\right)$$

Now using taylor expansion and approximating

$$\Rightarrow e^{\delta} = 1 + \delta + \frac{\delta^2}{2!} \cdots = 1 + \delta, \text{ for } \delta \to 0$$

$$\therefore \frac{\partial^2 \phi_{new}}{\partial X^2} = -\left(e^{-\phi_{old}}(1-\delta) - e^{\phi_{old}}(1+\delta) + C\right)$$

$$= -\left(e^{-\phi_{old}} - e^{\phi_{old}} + C\right) + \delta\left(e^{-\phi_{old}} + e^{\phi_{old}}\right)$$

$$\therefore \frac{\partial^2 \phi_{new}}{\partial X^2} - \phi_{new}\left(e^{-\phi_{old}} + e^{\phi_{old}}\right) = -\left[e^{-\phi_{old}} + e^{\phi_{old}} + C + \phi_{old}\left(e^{-\phi_{old}} + e^{\phi_{old}}\right)\right]$$

b) consider the following tri-diagonal matrix

$$\Rightarrow \quad A = \begin{bmatrix} a_1 & c_1 & & & \\ b_2 & a_2 & c_2 & & \\ & b_3 & \ddots & \ddots & \\ & & \ddots & \ddots & c_{n-1} \\ & & & b_n & a_n \end{bmatrix}$$

If we split this using LU decomposition

$$\Rightarrow \begin{bmatrix} 1 & 0 & 0 & \cdots & \\ \beta_2 & 1 & 0 & & \\ 0 & \beta_3 & 1 & & \\ 0 & & \ddots & & \\ \vdots & & & \beta_n & 1 \end{bmatrix} \begin{bmatrix} \alpha_1 & c_1 & & & \\ & \alpha_2 & c_2 & & \\ & & \ddots & \ddots & \\ & & & \ddots & c_{n-1} \\ & & & & \alpha_n \end{bmatrix} = \begin{bmatrix} a_1 & c_1 & & \\ b_2 & a_2 & \ddots & \\ & \ddots & \ddots & \ddots \\ & & & \end{bmatrix}$$

$\therefore$ From the above matrices we have

$\alpha_1 = a_1$

$$\left.\begin{aligned} \beta_2 \alpha_1 &= b_2 \\ \beta_3 \alpha_2 &= b_3 \end{aligned}\right\} \Rightarrow \quad \beta_k \alpha_{k-1} = b_k \qquad k = 2, 3 \ldots n$$

$$\left.\begin{aligned} \alpha_2 &= a_2 - \beta_2 c_1 \\ \alpha_3 &= a_3 - \beta_3 c_2 \\ &\vdots \end{aligned}\right\} \quad \alpha_k = a_k - \beta_k c_{k-1} \qquad k = 2, 3 \ldots n$$

Once α_1 is known all other terms can be found recursively and α_1 is known, since it is directly equal to a_1

Now from the analysis of part ⓐ we have

$$a^n \phi_{i+1}^{n+1} - b^n \phi_i^{n+1} + c^n \phi_{i-1} = f^n$$

This can be shown as a tri-diagonal matrix as follows

$$\overset{A}{\begin{bmatrix} \ddots & \ddots & & \\ \ddots & \ddots & \ddots & \\ a & b & c & \ddots \\ & \ddots & \ddots & \ddots \end{bmatrix}} \overset{\phi}{\begin{bmatrix} \vdots \\ \phi_{i-1} \\ \phi_i \\ \phi_{i+1} \\ \vdots \end{bmatrix}} = \overset{f}{\begin{bmatrix} \vdots \\ f_i \\ \vdots \end{bmatrix}}$$

∴ Now using LU decomposition we split the A matrix

$$\Rightarrow \overset{L}{\begin{bmatrix} 1 & & & & \\ \beta_2 & 1 & & & \\ & \beta_3 & 1 & & \\ & & \ddots & \ddots & \\ & & & \beta_n & \end{bmatrix}} \overset{U}{\begin{bmatrix} \alpha_1 & c_1 & & & \\ & \alpha_2 & c_2 & & \\ & & \ddots & \ddots & \\ & & & c_{n-1} & \\ & & & \alpha_n & \end{bmatrix}} \overset{\phi}{\begin{bmatrix} \phi_1 \\ \phi_2 \\ \vdots \\ \phi_n \end{bmatrix}} = \overset{f}{\begin{bmatrix} f_1 \\ f_2 \\ \vdots \\ f_n \end{bmatrix}}$$

Now to solve this we first combine U and ϕ

$$\Rightarrow Z = U\phi$$

$$\Rightarrow \overset{L}{\begin{bmatrix} 1 & & & & \\ \beta_2 & 1 & & & \\ & \beta_3 & 1 & & \\ & & \ddots & \ddots & \\ & & & \beta_n & 1 \end{bmatrix}} \overset{Z}{\begin{bmatrix} z_1 \\ z_2 \\ \vdots \\ z_n \end{bmatrix}} = \overset{f}{\begin{bmatrix} f_1 \\ \vdots \\ f_n \end{bmatrix}}$$

From this we get $z_1 = f_1 \implies z_1$ known

$z_1 \cdot \beta_2 + z_2 = f_2 \implies z_2$ found

$z_2 \beta_3 + z_3 = f_3$

$\therefore$ we can recursively find the values of all z_i since we know all the f_i and β_i

Now that we know z_i

$$z = U\phi \implies \begin{bmatrix} \alpha_1 & c_1 & & \\ & \alpha_2 & c_2 & \\ & & \ddots & \ddots \\ & & & c_{n-1} \\ & & & \alpha_n \end{bmatrix} \begin{bmatrix} \phi_1 \\ \phi_2 \\ \vdots \\ \phi_n \end{bmatrix} = \begin{bmatrix} z_1 \\ z_2 \\ z_3 \\ \vdots \\ z_n \end{bmatrix}$$

Now, looking from the bottom up $\implies \alpha_n \phi_n = z_n$

$$\left\{ \begin{array}{l} \alpha_{n-1}\phi_{n-1} + c_n \phi_n = z_{n-1} \\ \alpha_{n-2}\phi_{n-2} + c_{n-1}\phi_{n-1} = z_{n-2} \end{array} \right.$$

Here also we can recursively solve upwards to the find the values of ϕ_i (z_i, α_i, c_i are known)

$\therefore$ The LU decomposition allows us to find the ϕ values for each iteration without requirement of inverse. This method is faster and simple.

Q1 Solution

a. Flow Chart Summary:

A. Background/Challenge:

- Investigating FinFET design considerations using 3D simulations and an analytical model. The essential aim of the paper is to create a methodology to encompass additional variations of fully depleted devices, with the formulation of corresponding design equations.

B. Problem Statement:

- As a step towards the larger goal of creating a general methodology, the authors carry out 3D simulations of the short-channel effects in the subthreshold region of the FET and then analytically solve the same setup to see the differences in the two methodologies.

C. **Proposal:**

- The analytical solution involves assuming the Laplace equation for the analysis. The design equations for the subthreshold behaviour in fully depleted silicon fins are derived using an analytical solution of the 3-D Laplace's equation.

- To simplify computations, the paper considers the condition where the fin height (H_fin) significantly exceeds the fin thickness (T_fin). Additionally, assumptions like a fixed location of the lowest barrier potential and calibration using 3D simulation results are outlined.

D. **Validation:**

- The proposed solution undergoes validation through two main avenues: 3D simulations and comparing previously reported results. The validation process aims to ensure that the analytical model aligns closely with experimental and numerical findings, enhancing the credibility of the proposed solution.

E. **Impact of Solution:**

- The paper concludes by emphasising the practical significance of the developed analytical solution. It provides close-form solutions for Short-channel effects in the subthreshold region of FinFETs. These solutions offer valuable insights and can serve as a starting point for obtaining initial values in device specifications.

b. Assumptions and Validity:

- Coulomb Scattering: There is doubt about the validity of using the mobility model for FinFET simulation calibrated using bulk CMOS. When the gate oxide thickness is smaller than 2.5 nm [30], long-range Coulomb scattering becomes noticeable, and the mobility model does not account for this feature.

- Velocity saturation: Velocity overshoot can be significant for channel lengths shorter than 60 nm; however, only velocity saturation is considered here. Thus, the threshold current must be more precise to provide a quantitative analysis.

- Doping and Carrier Concentration: Ignoring potential perturbations due to doping and carrier concentration simplifies the model but may overlook important factors.

- Buried Oxide Sensitivity: The buried oxide is assumed to be sufficiently thick to provide a negligible electric field when there is a finite potential across it.

- Homogeneity : By substituting the effective dimensions for the physical dimensions, the barriers between the silicon fin and gate oxide are erased. Effective thickness, effective channel length, and effective height are computed for the entire region, treating it as homogenous silicon.

- Leakage Current Path: Assuming leakage current is dominated by the most leaky path, not integrated, simplifies calculations but may oversimplify the actual current distribution.

- Lowest Barrier Location: Fixing the lowest barrier location streamlines the analysis but may not hold in all scenarios.

- Temperature Independence: The model assumes temperature independence, acknowledging this assumption and discussing its impact on its validity would be beneficial.

Comment: These assumptions collectively simplify the model, making it more tractable for analysis but introduce potential limitations in representing real-world complexities.

d. Benefits of the Paper:

The paper provides both qualitative insights and reasonably accurate approximations for the quantitative relationship between device geometry and performance in the sub-threshold region of FinFETs. This analysis offers a solid foundation for extending the findings to other transistor designs such as DGFET and FDFET, provided appropriate assumptions are made. The presented analytical method enables efficient derivation of approximate results, facilitating deeper understanding and streamlined computations for researchers and engineers working in this domain. Additionally, the paper's approach allows for potential further exploration and application in related areas of semiconductor device engineering and design optimization.

e. Understanding of the Paper:

The paper focuses on device geometry and short channel effects in the sub-threshold area of FinFETs. In order to fully comprehend other terminologies, such quantization impact and scaling effects, more research is required. The paper's analytical elements were delivered clearly and effectively. The presumptions made were reasonable and supported by strong evidence. However, the concept's application to similar H_fin and T_fin dimensions is still a little unclear. Furthermore, understanding the geometric approximation of H_eff and T_eff was difficult and required additional clarification.

f. Analysis for paper 2

Metal gate granularity (MGG) is the main cause of variability in FinFETs. Studying its impacts on circuits necessitates the use of an analytical model to comprehend its impact on threshold voltage.

6c Solution

PART 1 : Na = 1e17, Nd = 1e17

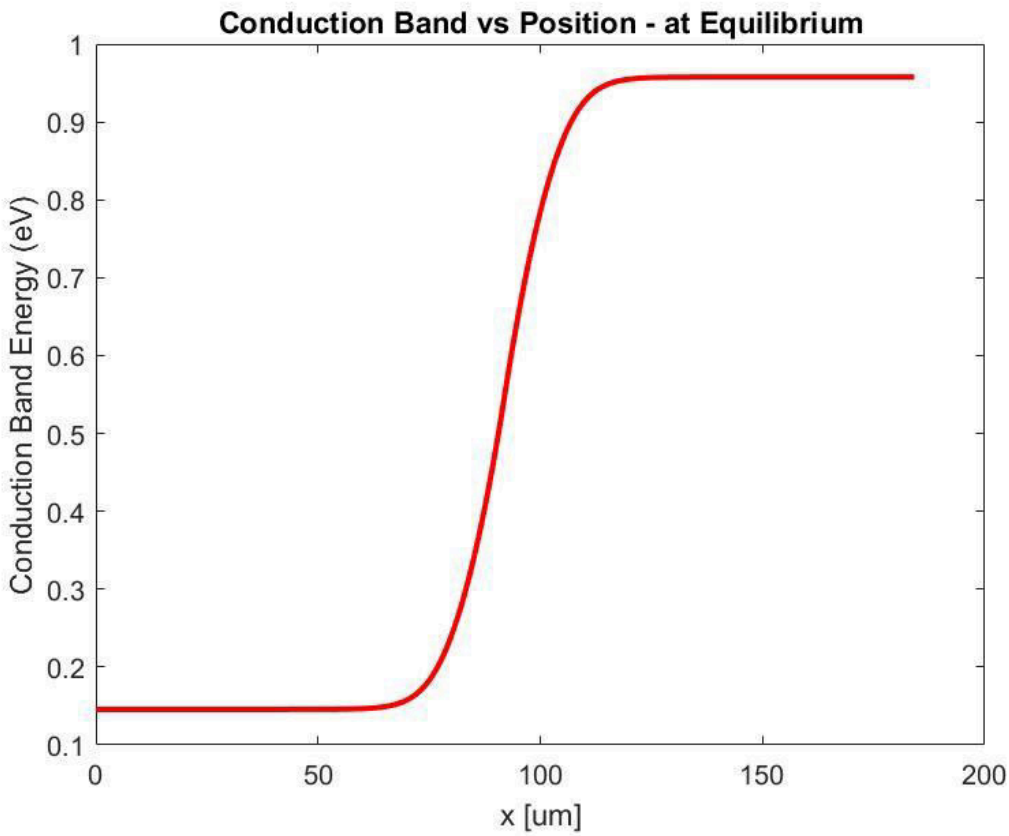

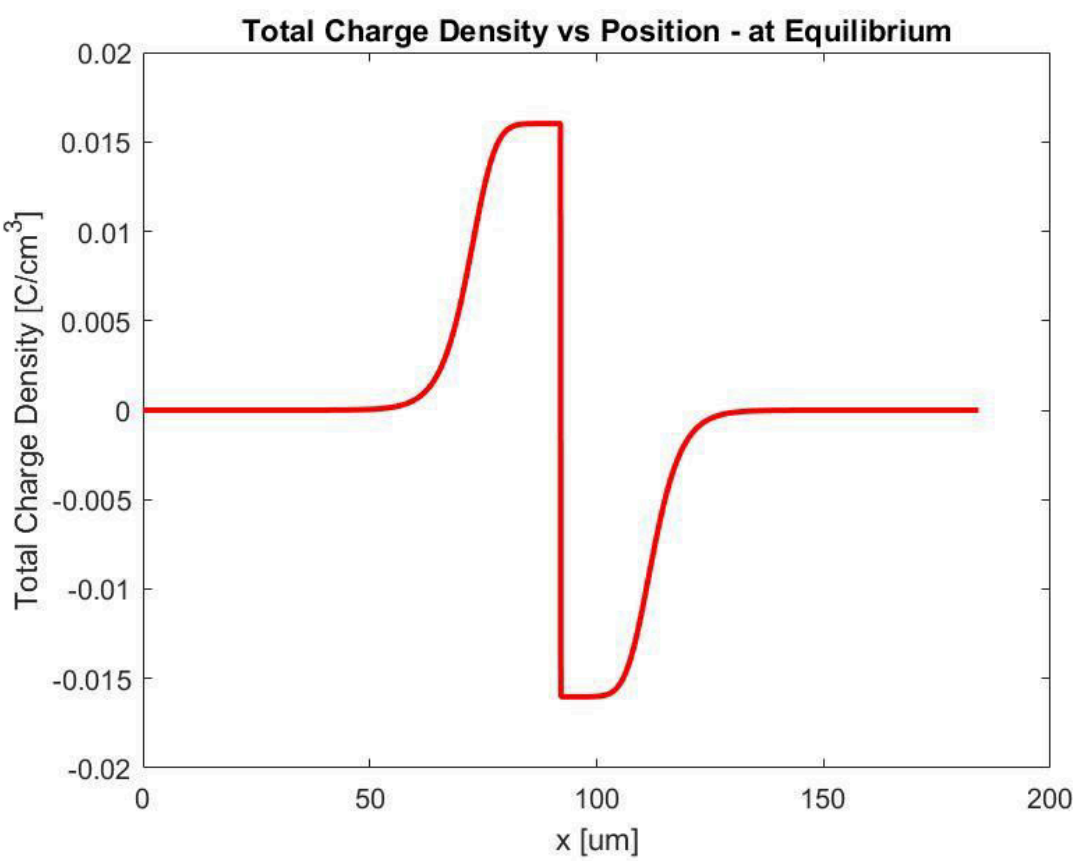

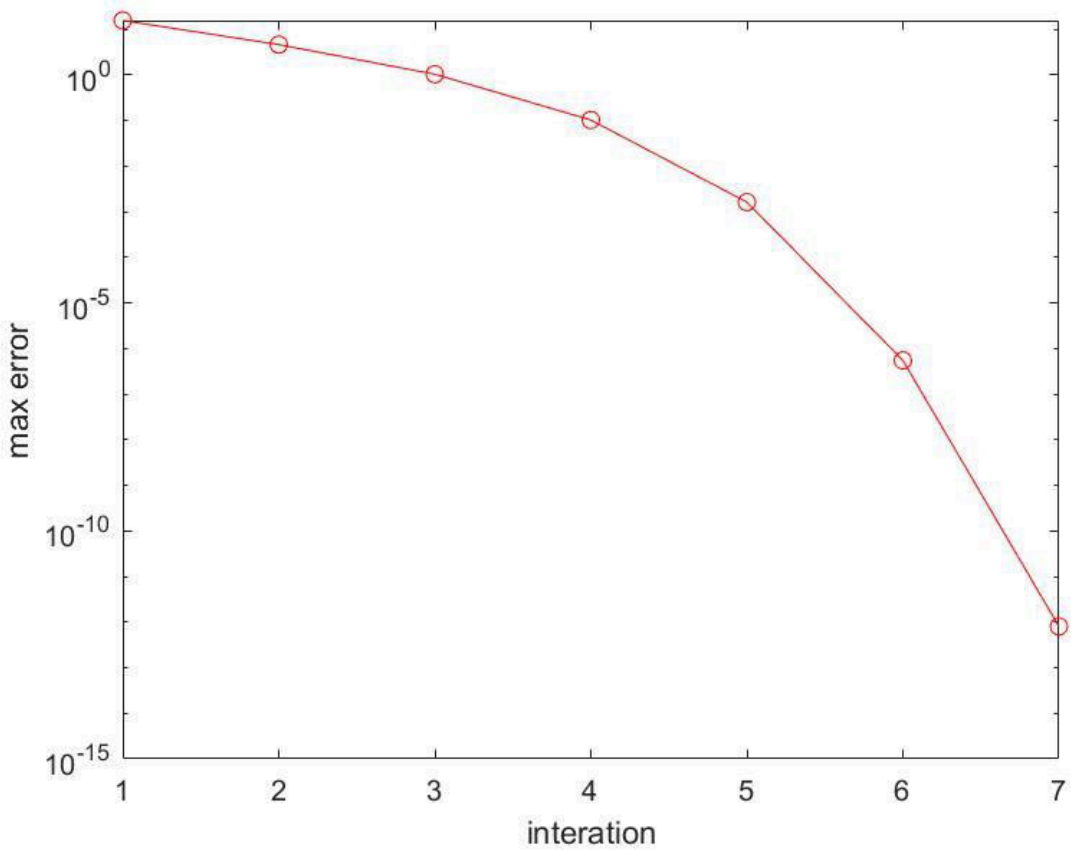
max error
interation
10^{0}
10^{-5}
10^{-10}
10^{-15}
1
2
3
4
5
6
7

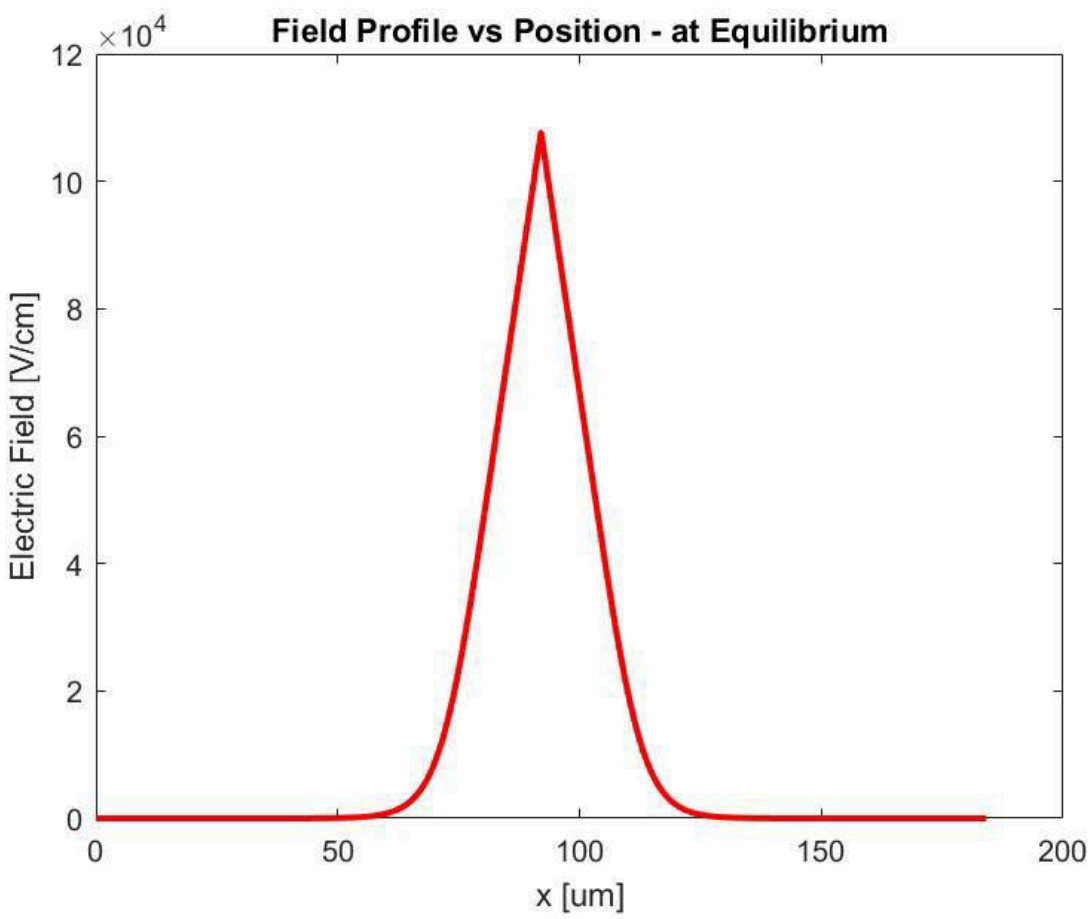
Field Profile vs Position - at Equilibrium
$\times 10^{4}$
Electric Field [V/cm]
x [um]
0
2
4
6
8
10
12
0
50
100
150
200

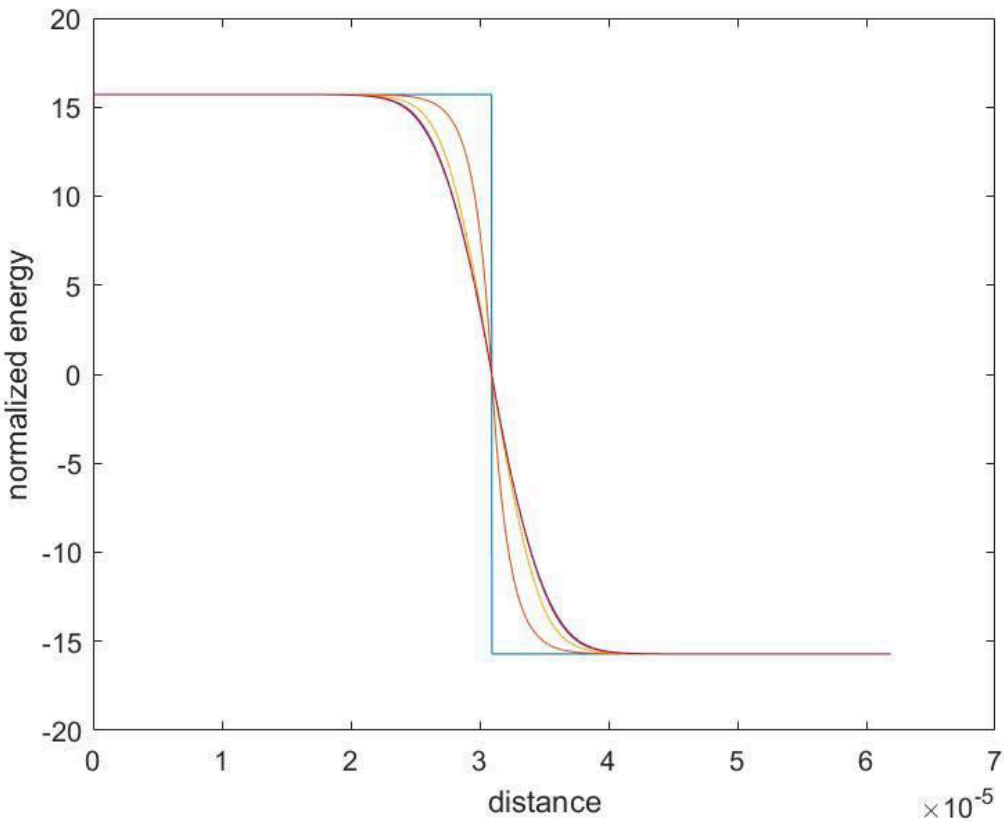
normalized energy
distance
×10^-5
20
15
10
5
0
-5
-10
-15
-20
0
1
2
3
4
5
6
7

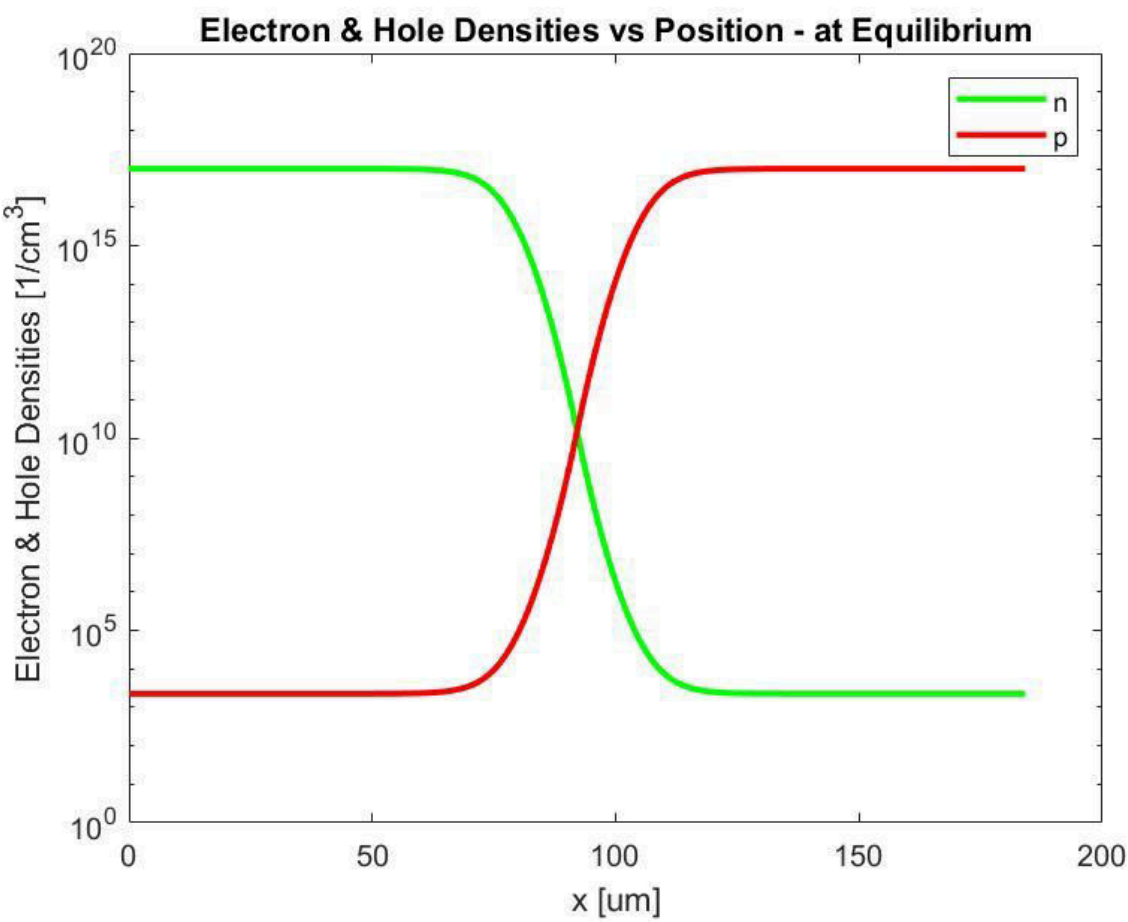
Electron & Hole Densities vs Position - at Equilibrium
Electron & Hole Densities [1/cm^3]
x [um]
n
p
10^20
10^15
10^10
10^5
10^0
0
50
100
150
200

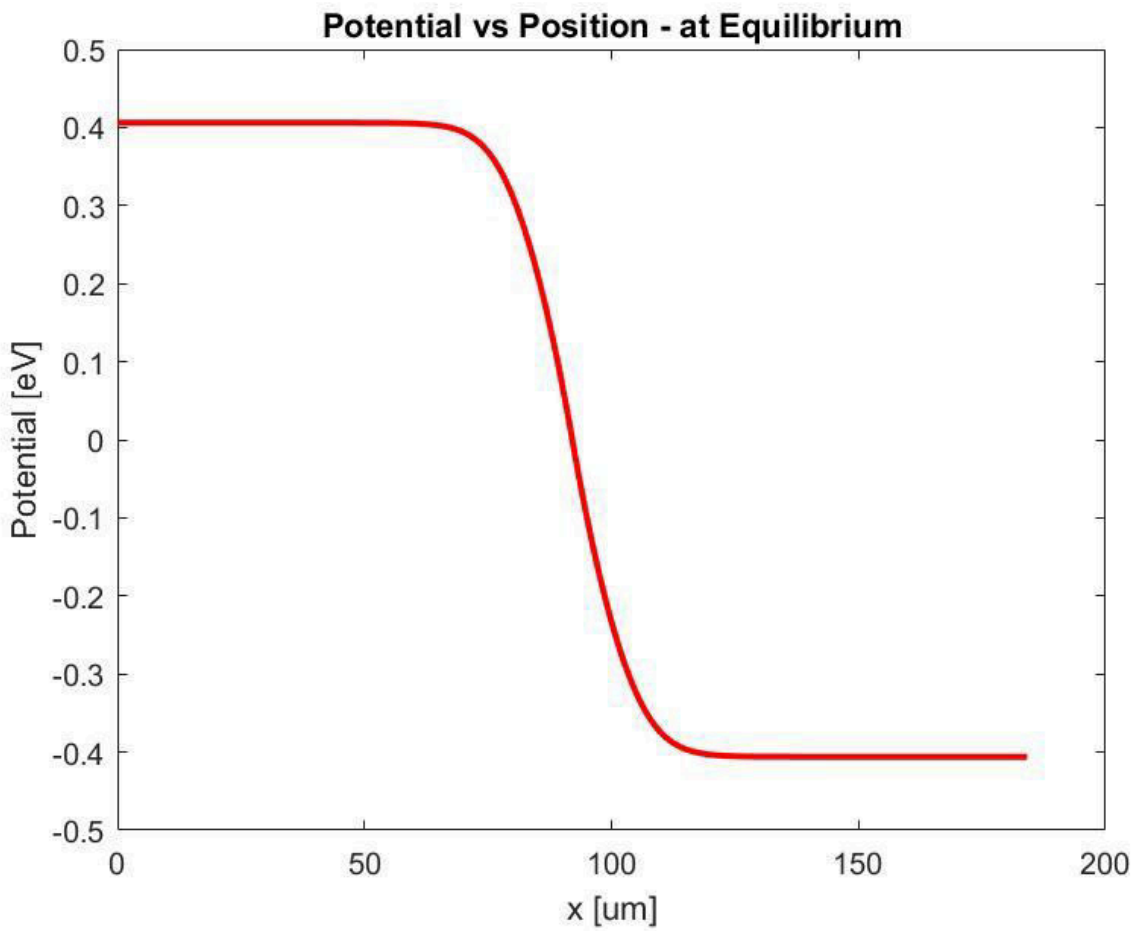

Main locations of deviation from depletion approximation :

We can see in the diagram of the total charge density that total charge density does not become zero immediately after or before the specific distance from the interface, i.e. the positive and negative charge profiles in the p and n regions are not perfect rectangles, hence, they violate the depletion approximation.

Observed shape of the n and p profiles and the potential profile :

The n and p profiles are symmetric about the interface because the doping of the n and p sides is equal. The same applies to the potential profile. Also, the maximum absolute potential of the n and p sides are equal.

PART 2 : Na = 1e17, Nd = 1e16

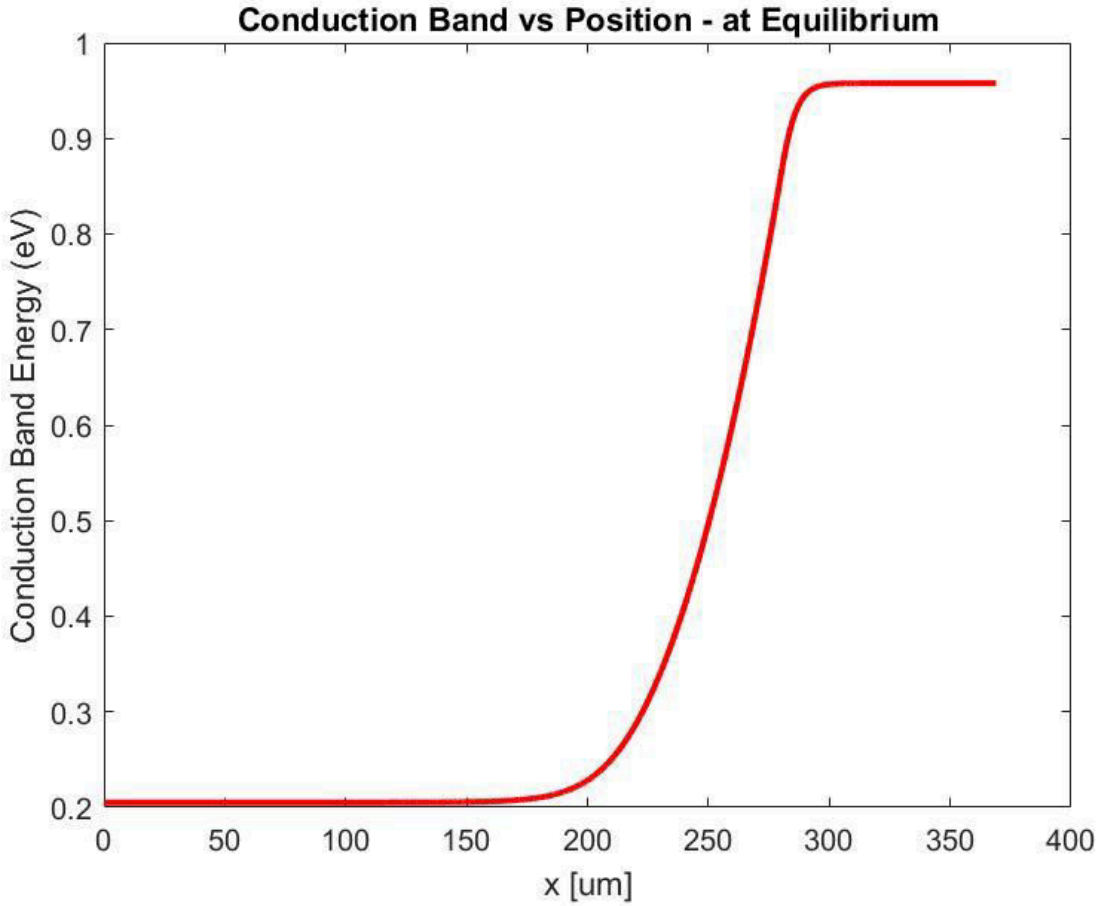

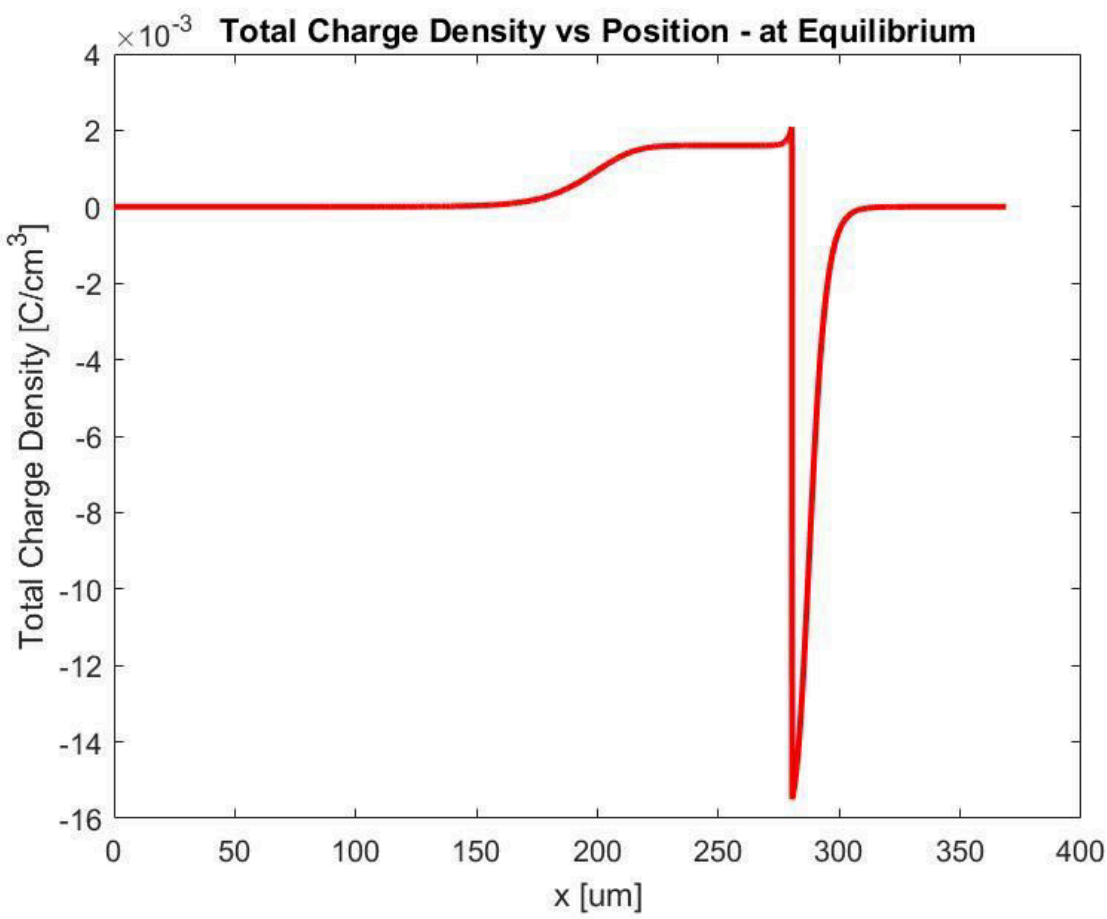

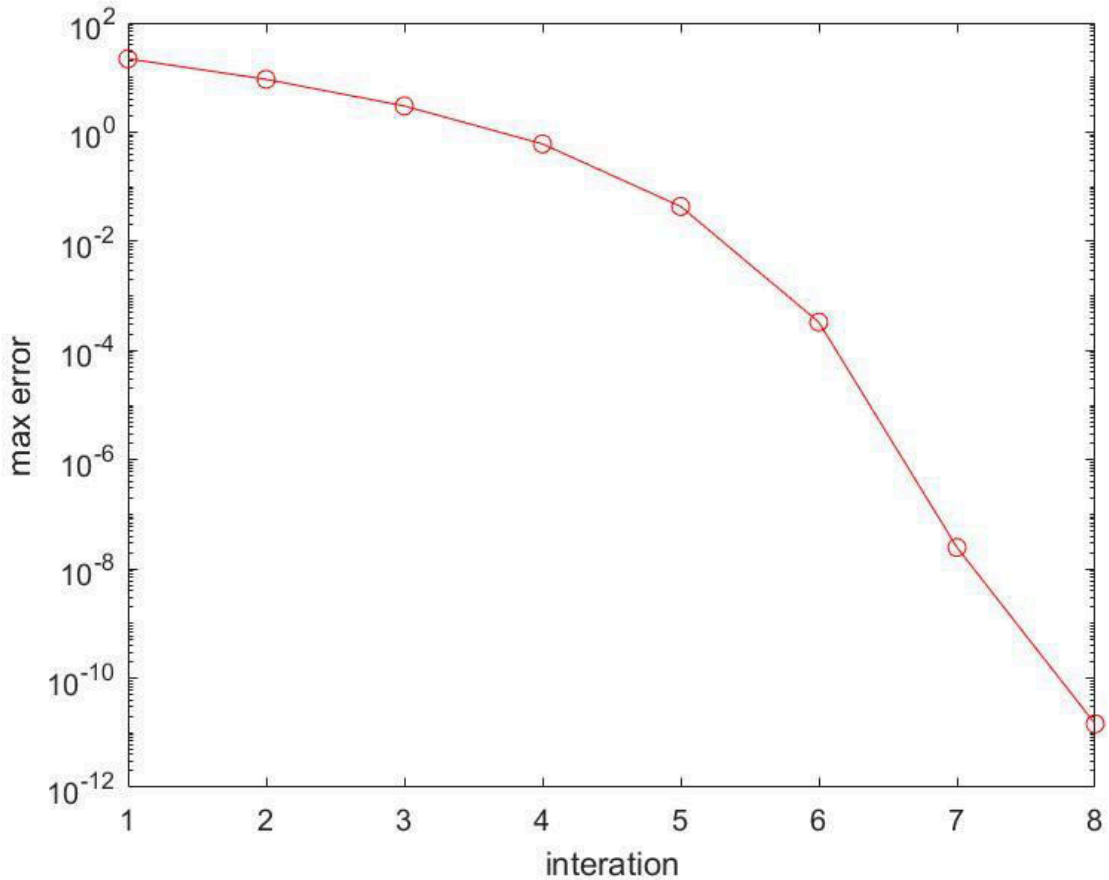
max error
interation
10^{2}
10^{0}
10^{-2}
10^{-4}
10^{-6}
10^{-8}
10^{-10}
10^{-12}
1
2
3
4
5
6
7
8

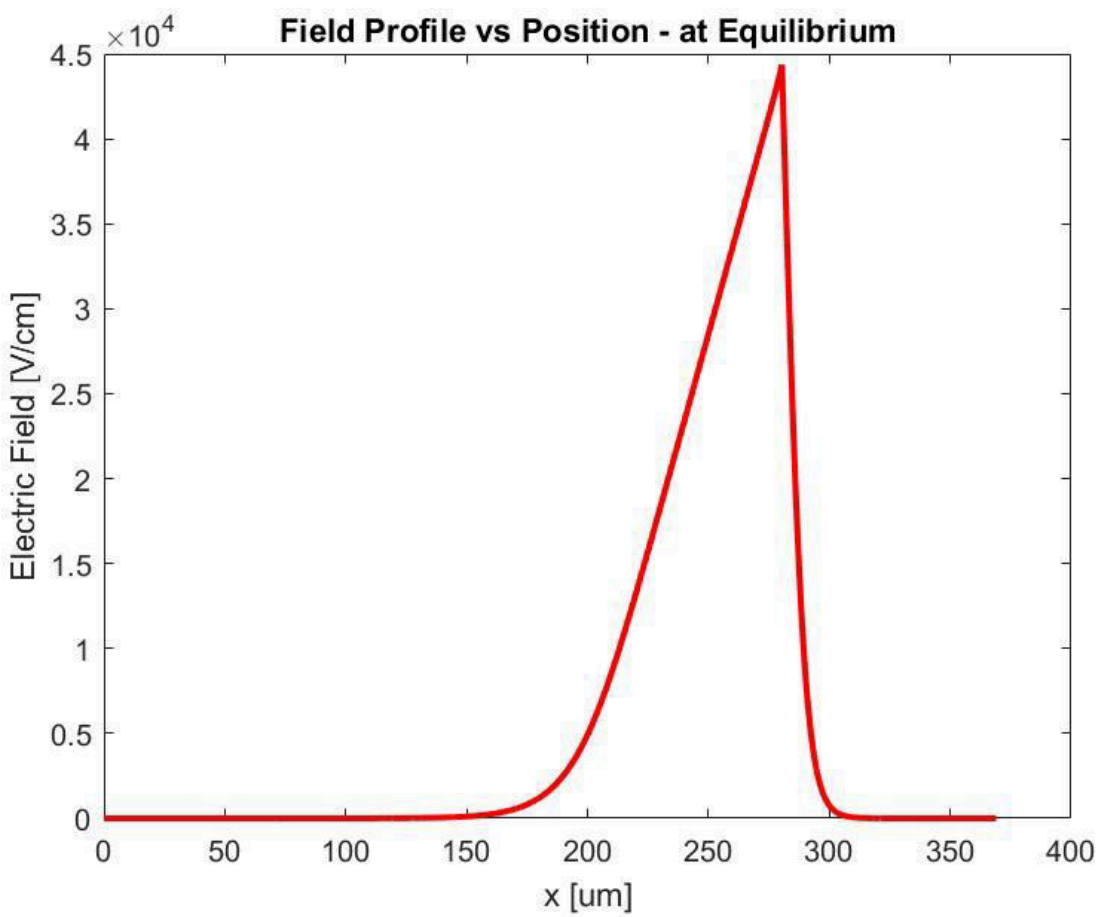
Field Profile vs Position - at Equilibrium
$\times 10^{4}$
Electric Field [V/cm]
x [um]
4.5
4
3.5
3
2.5
2
1.5
1
0.5
0
0
50
100
150
200
250
300
350
400

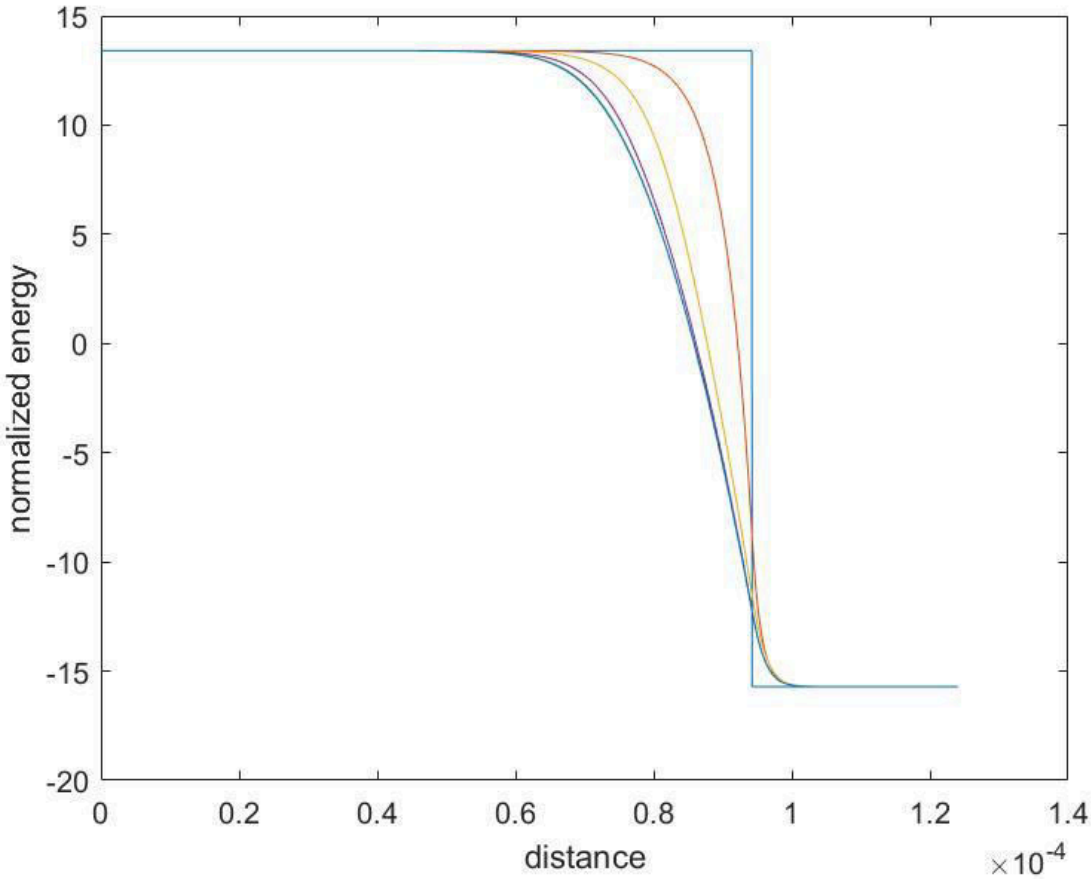
15
10
5
0
-5
-10
-15
-20
normalized energy
0
0.2
0.4
0.6
0.8
1
1.2
1.4
distance
×10^-4

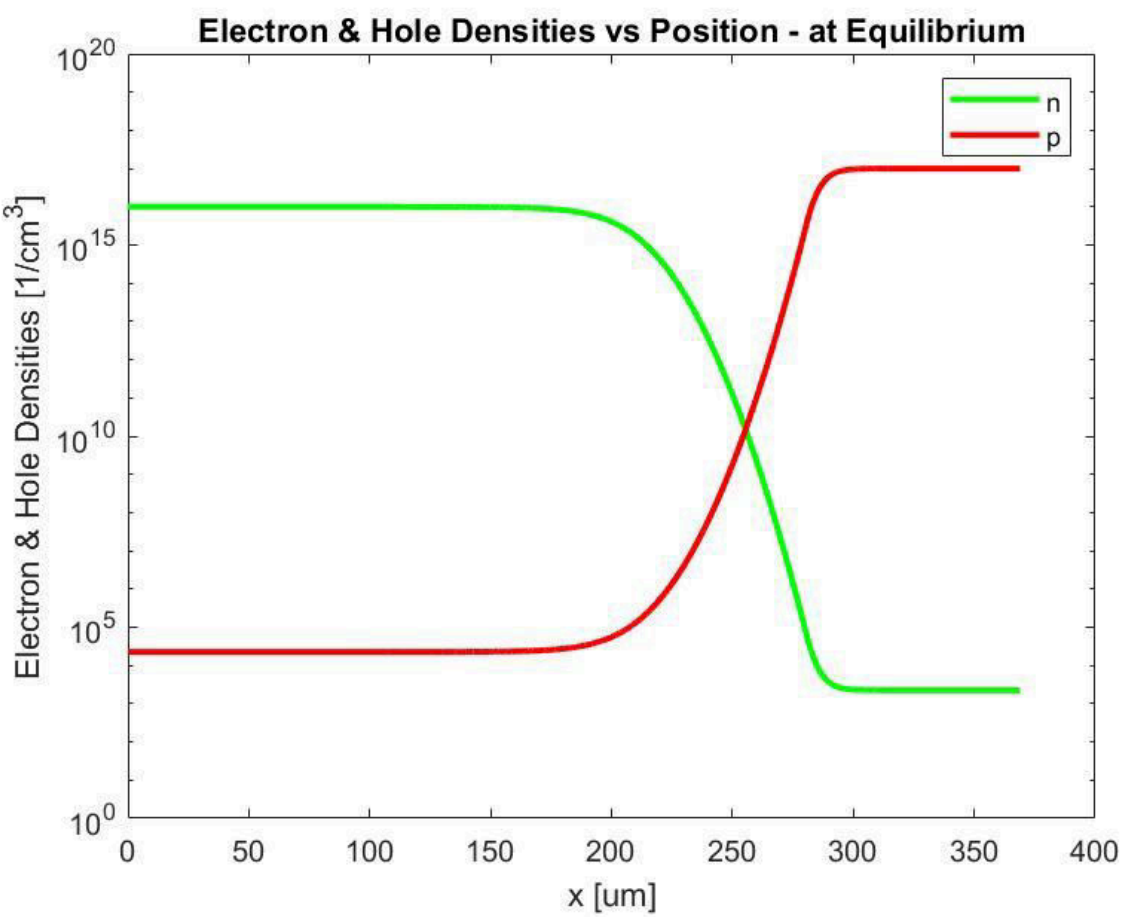
Electron & Hole Densities vs Position - at Equilibrium
n
p
10^20
10^15
10^10
10^5
10^0
Electron & Hole Densities [1/cm^3]
0
50
100
150
200
250
300
350
400
x [um]

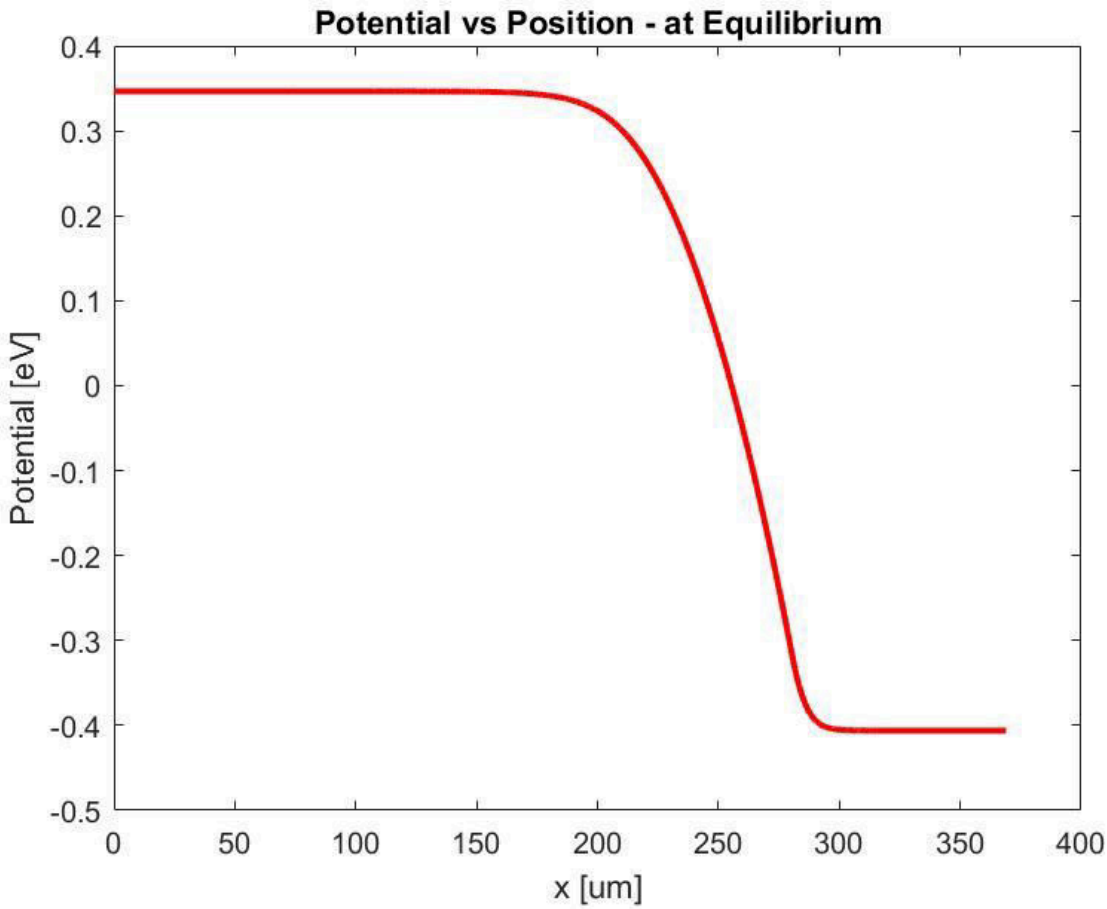

Comparison of the two profiles and explanation of the notch

The V profile for the second case is similar in shape to the first case but is slightly shifted towards the right because of the difference in the doping concentration. Essentially, the depletion layer forms more into the n region.

The notch is formed because as the doping concentrations become unequal, the depletion region moves towards the side with less doping. Hence, the point where the n concentration drops and p increases is shifted from the centre, whereas the Na and Nd concentration profiles are fixed. This mismatch causes he fixed charges to create a notch at the point where the n and p charges cancel each other.

PART 3: Boundary conditions

The boundary conditions are given by the following part of the code

```
a(1) = 0;
c(1) = 0;
b(1) = 1;
f(1) = fi(1);
a(n_max) = 0;
c(n_max) = 0;
b(n_max) = 1;
f(n_max) = fi(n_max);
```

The boundary conditions are justified by deriving the relation of the terms in the LU decomposition used in the code later. a and c have zero initial and final values since the contact at the ends of the junction being studied is ohmic and, therefore, has zero phi (Ef = Ec). Also, the f boundary conditions are justified since the potentials at the first and last grid points are the potentials at the start and end of the junction.

PART 4: Mesh Definition

The region where the mesh is defined is

```
xx1(1) = dx*1e4;

   Ec = dEc - Vt*fi;     %Values from the second Node%
   ro = -ni*(exp(fi) - exp(-fi) - dop);
   el_field1 = -([fi 0 0] - [0 fi 0])*Vt/(dx*Ldi);
   el_field2 = -([fi 0 0] - [ 0 0 fi])*Vt/(2*dx*Ldi);
   n = exp(fi);
   p = exp(-fi);
   xx1 = x.*1e4/Ldi;

   el_field1 = el_field1(2: n_max+1);
   el_field2 = el_field2(2: n_max+1);

Ec(1) = Ec(2);
Ec(n_max) = Ec(n_max-1);
xx1(n_max) = xx1(n_max-1) + dx*Ldi*1e4;
el_field1(1) = el_field1(2);
el_field2(1) = el_field2(2);
el_field1(n_max) = el_field1(n_max-1);
el_field2(n_max) = el_field2(n_max-1);
n(n_max)=n(n_max-1);
p(n_max)=p(n_max-1);
```

- A uniform mesh choice is valid because we did not know the profile of the potential or doping being calculated. Hence, if we take a non-uniform mesh, it could affect the precision of the profile calculation. We can take a non-uniform mesh, with the mesh being more dense in regions of faster variation of the parameter, but only if we have some preliminary analytical idea of the profile of the parameter.
- Thus, if we use non-uniform meshing, we can reduce the number of meshing points without affecting the precision of the output by ensuring that regions with faster or more complex changes in the parameter have a finer mesh than other regions.

PART 5: Error in the initial guess solution

The error in the initial guess solution was because it was based on the ideal analytical solution, which considered the depletion approximation. To get a realistic solution, we must numerically solve the exponential dependence in the second-order differential equation with the starting point as the guess solution. Therefore, we need multiple iterations to decrease the error between what we predict using the differential equations and our solution.

PART 6: Initial guess profile

The code which creates the initial guess solution is

```
x=[0:dx:x_max];

if profile==1
yn=(x<LLn|x>LLn+LLp);       % n region is defined for npn%
<<<<<<<<<<<<<<<<<<<<<<<NPN<<<<<<<<<<<<<<<<
else
   yn=(x<nfactor*Wn);       % n region is defined %
<<<<<<<<<<<<<<<<<<<<<<<PN<<<<<<<<<<<<<<<<
end
yp=ones(1,n_max)-yn;      % p region is defined
dop=yn*Nd/ni- yp*Na/ni;     % defining doping at grid points

figure (1); plot(x, dop);
```

To get a linear variation, we change the code as follows:

```
x=[0:dx:x_max];

if profile==1
yn=(x<LLn|x>LLn+LLp);       % n region is defined for npn%
<<<<<<<<<<<<<<<<<<<<<<<NPN<<<<<<<<<<<<<<<<
```

```
else
   yn=(x<nfactor*Wn);       % n region is defined %
<<<<<<<<<<<<<<<<<<<<<<<PN<<<<<<<<<<<<<<<<
end
yp=ones(1,n_max)-yn;      % p region is defined
dop=  exp(x).*(yn*Nd/ni+ yp*Na/ni);     % defining doping at grid points

figure (1); plot(x, dop);
```

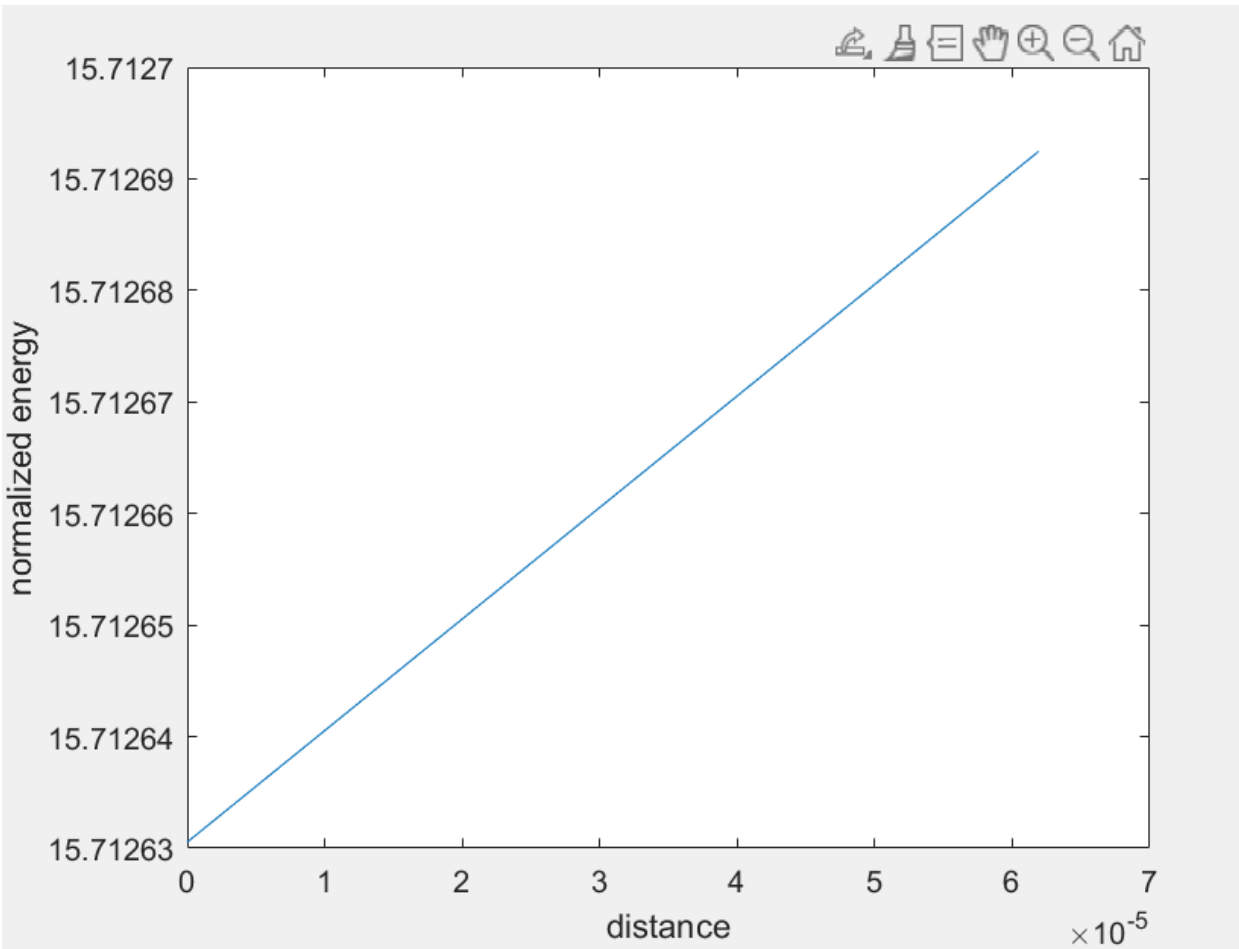

On the given code, I could not suitably change the UGEstatistics code to run the iterative solver since it stopped after the first iteration. But this method of using a different initial guess will work over some finite level of iterations because the error factor will eventually change the profile to match the analytical solution.

PART 7: NPN and NIN simulations

NPN Simulations

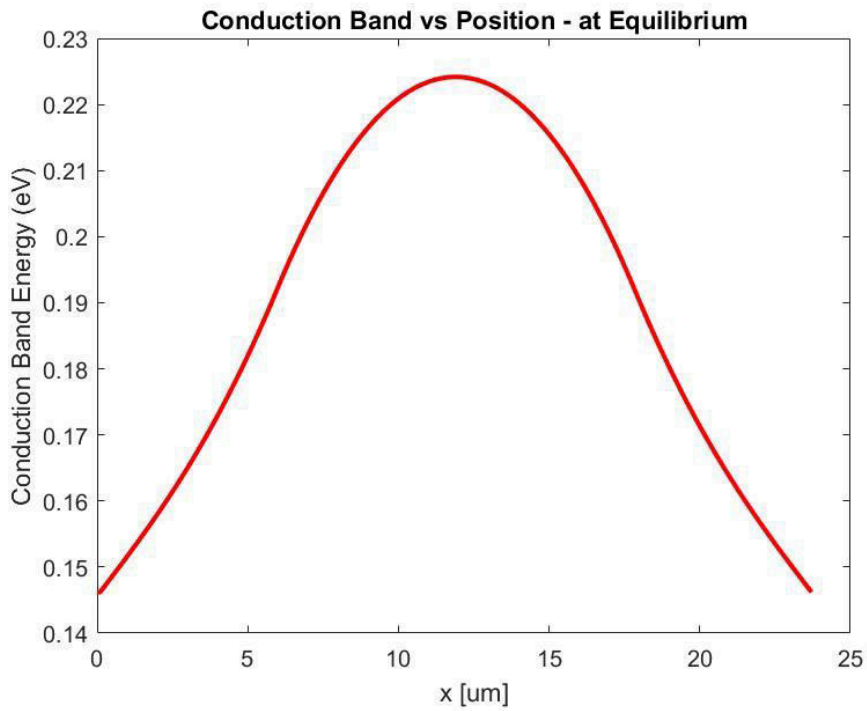

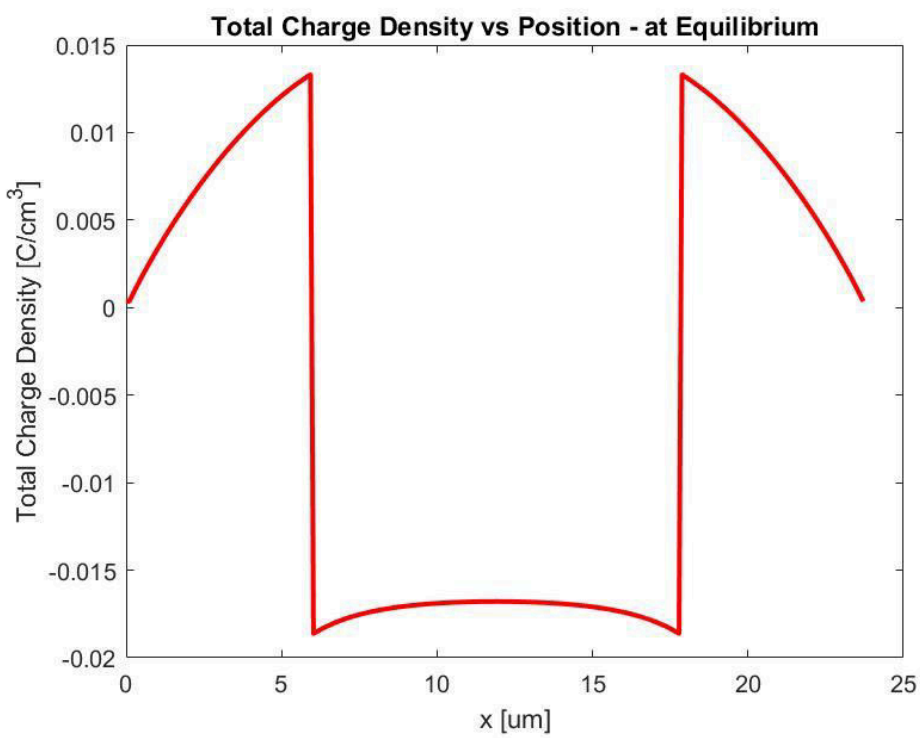

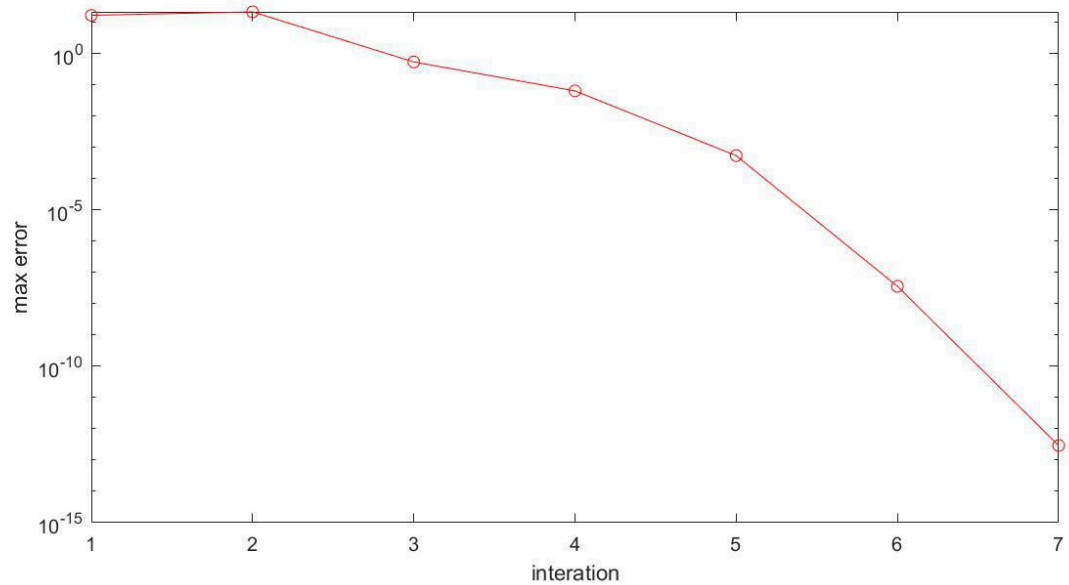
max error
interation
10^{0}
10^{-5}
10^{-10}
10^{-15}
1
2
3
4
5
6
7

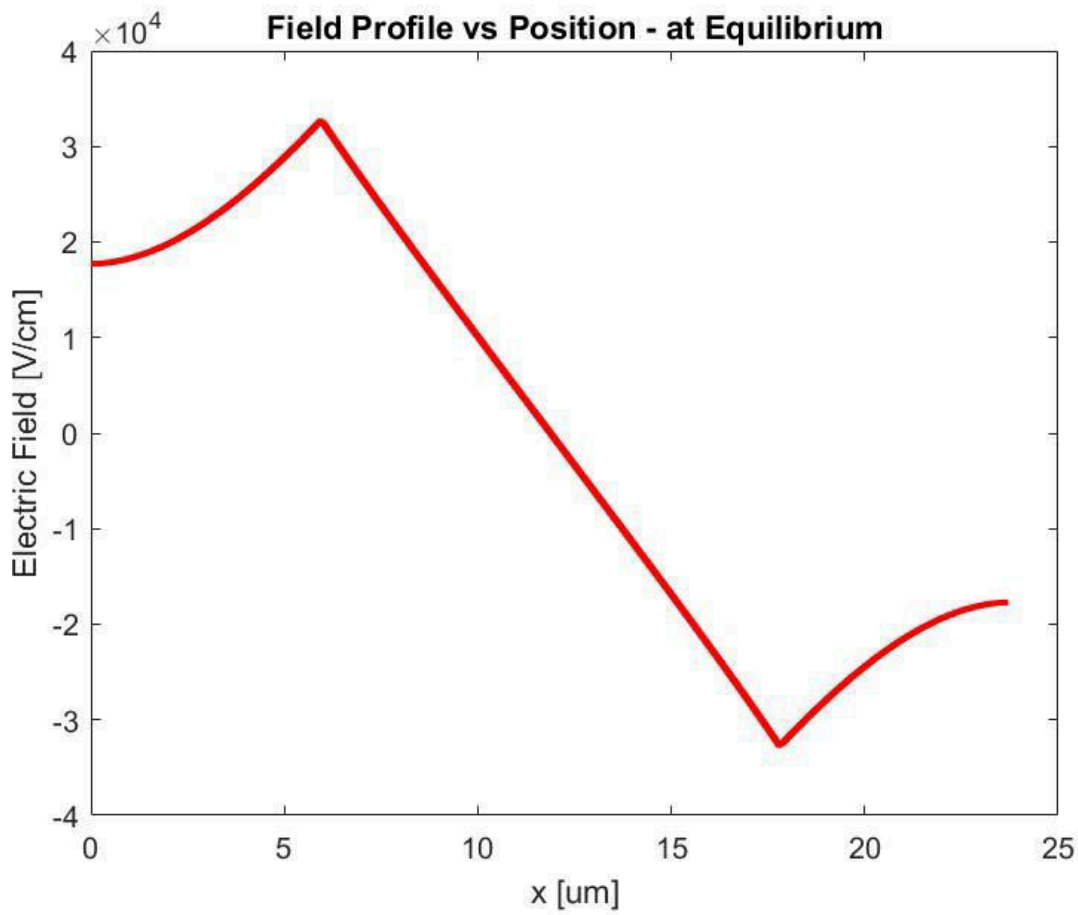
Field Profile vs Position - at Equilibrium
$\times 10^{4}$
Electric Field [V/cm]
x [um]
4
3
2
1
0
-1
-2
-3
-4
0
5
10
15
20
25

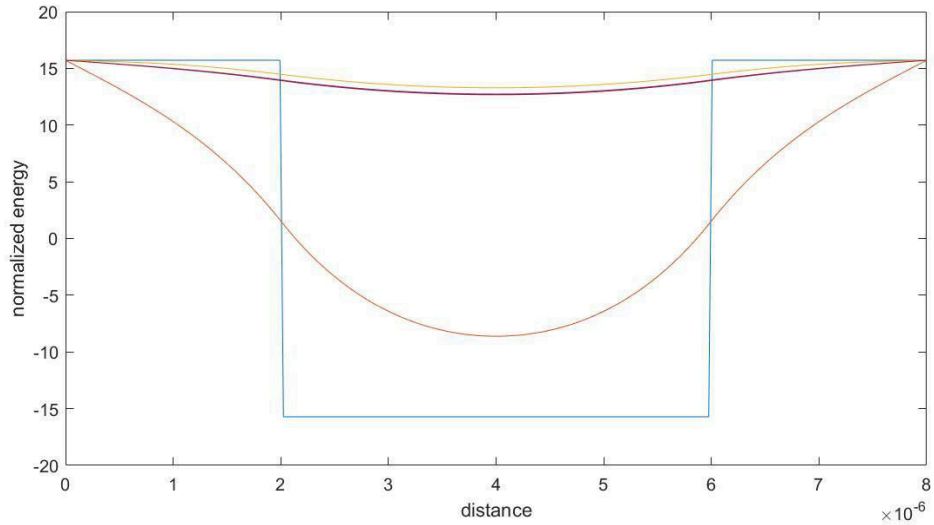
normalized energy
distance
×10^-6

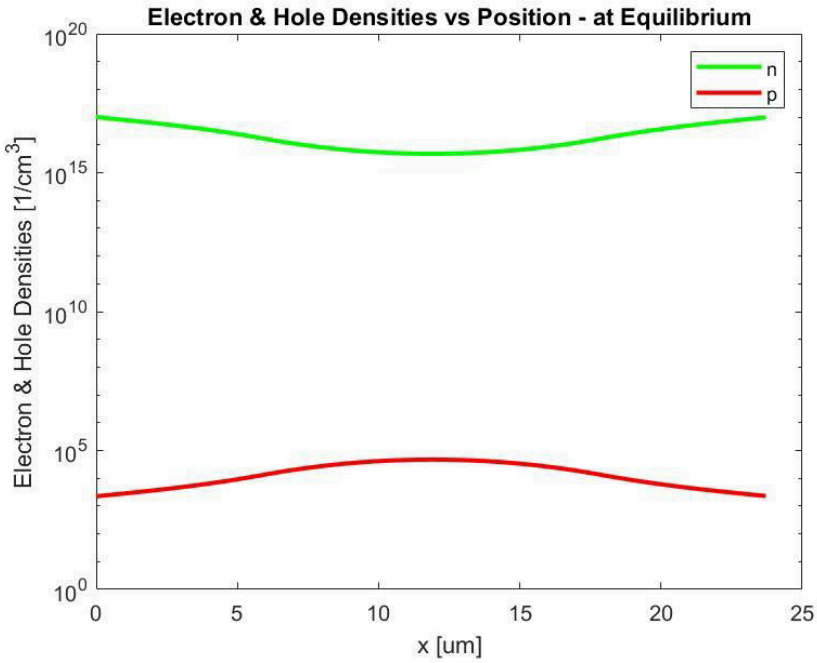
Electron & Hole Densities vs Position - at Equilibrium
Electron & Hole Densities [1/cm^3]
x [um]
n
p

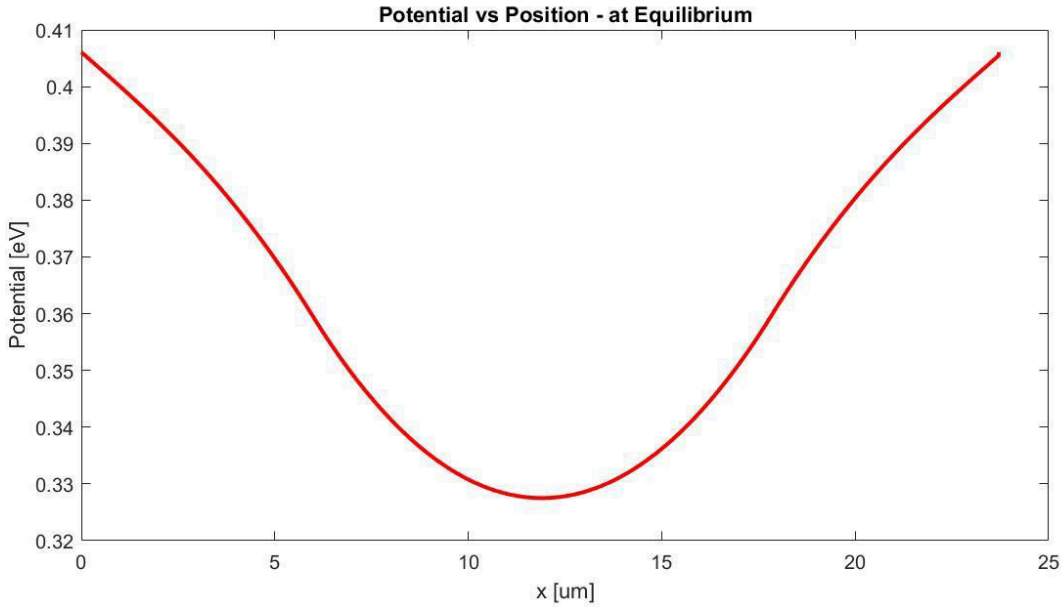
Potential vs Position - at Equilibrium
Potential [eV]
x [um]

Variation of barrier height with doping for NPN

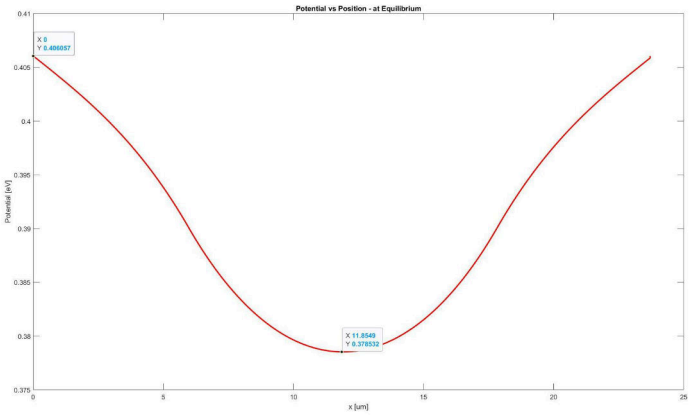

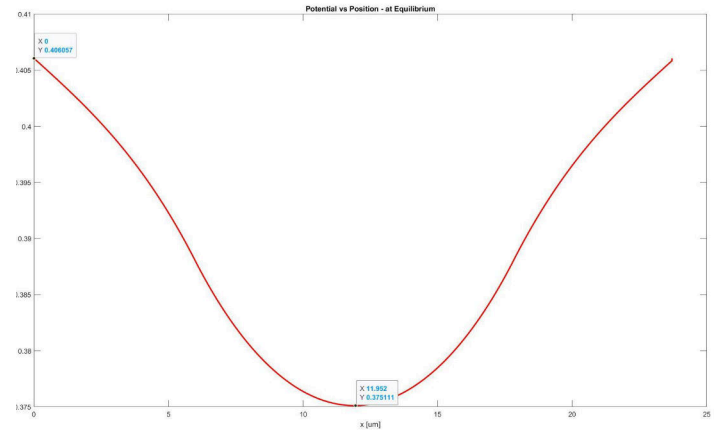

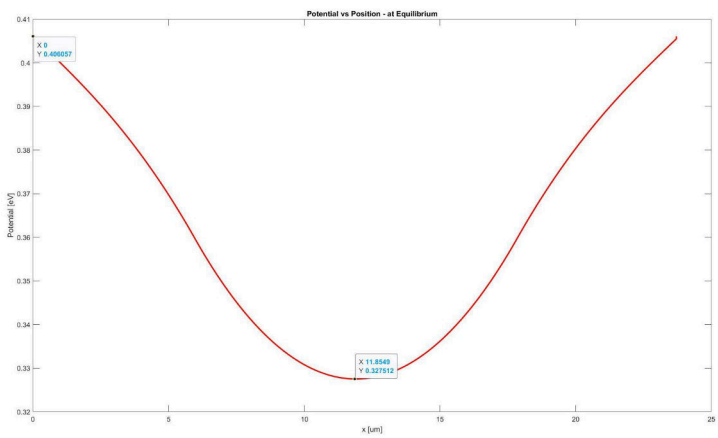

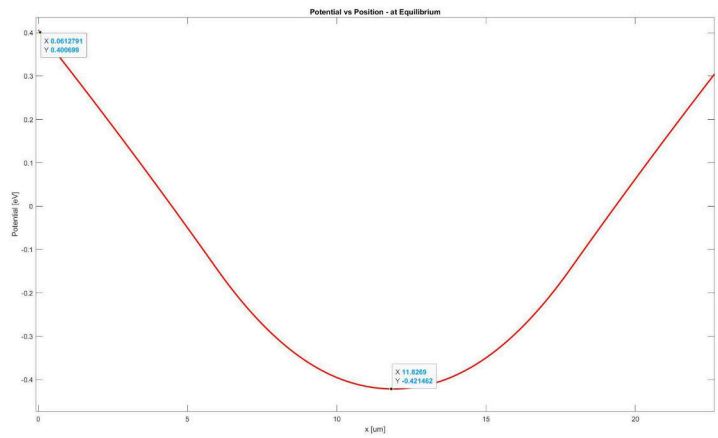

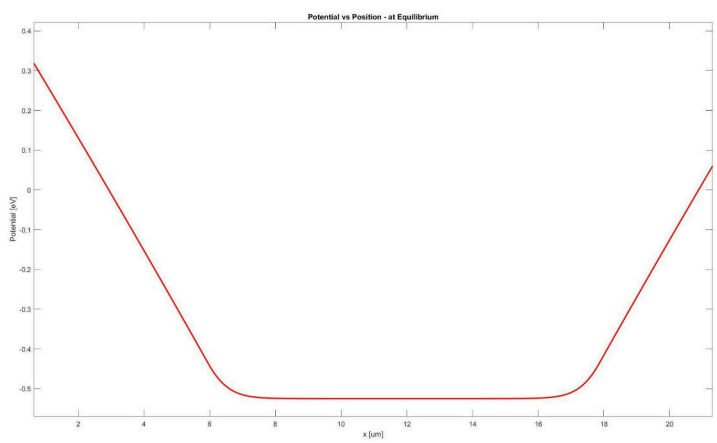

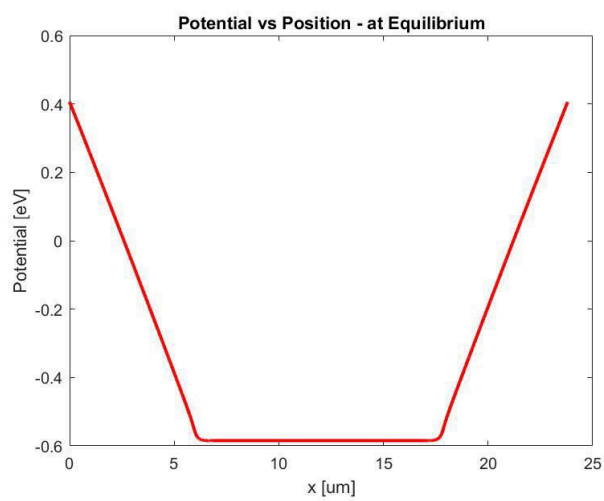

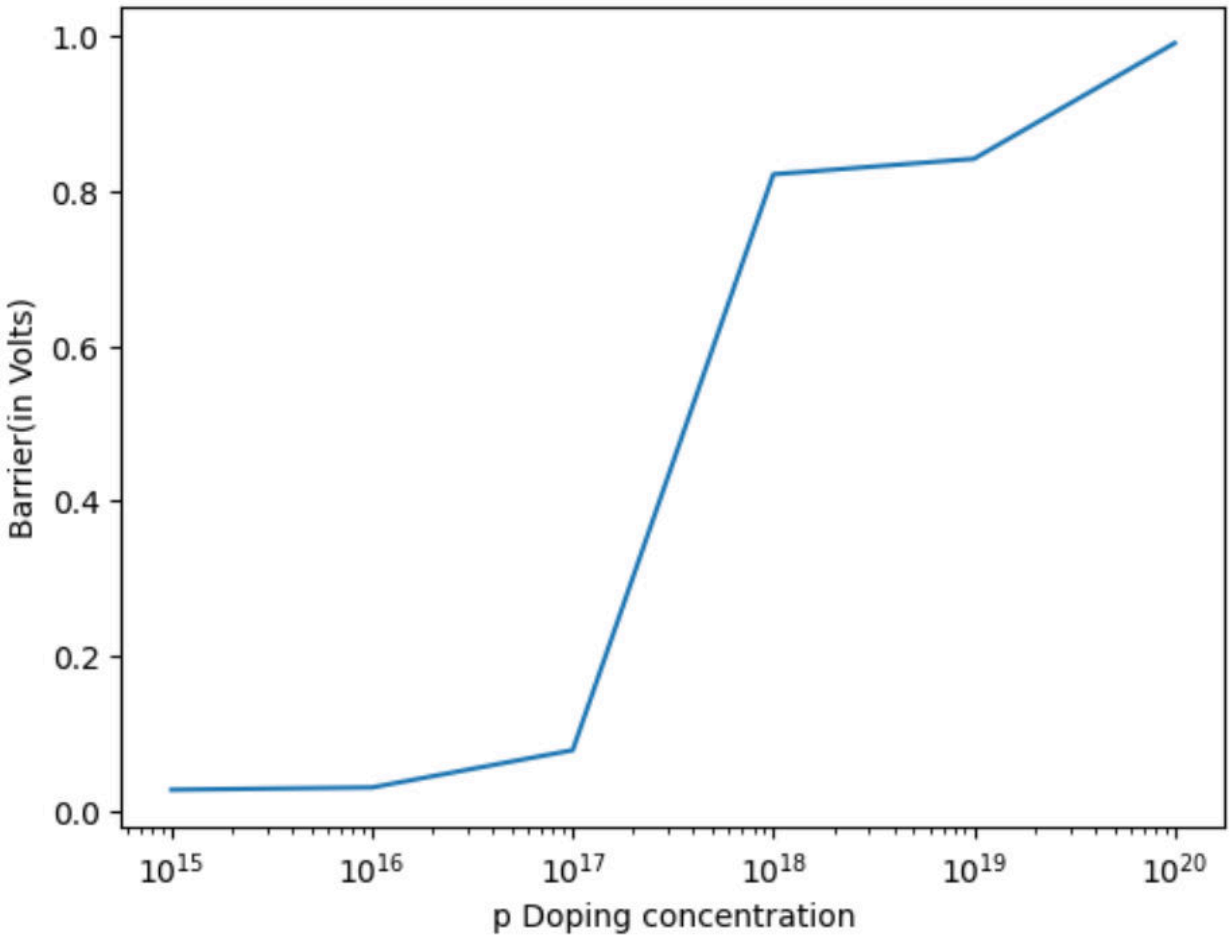

The barrier height increases rapidly as the p doping crosses over n doping. This is because when the p concentration becomes more than the n concentration, the depletion region primarily resides within the n-type region. This situation resembles a metal-semiconductor contact, forming a Schottky barrier at the interface. The work function difference and the dopant concentration (p) in the p-type region influence the Schottky barrier height.

NIN Simulations

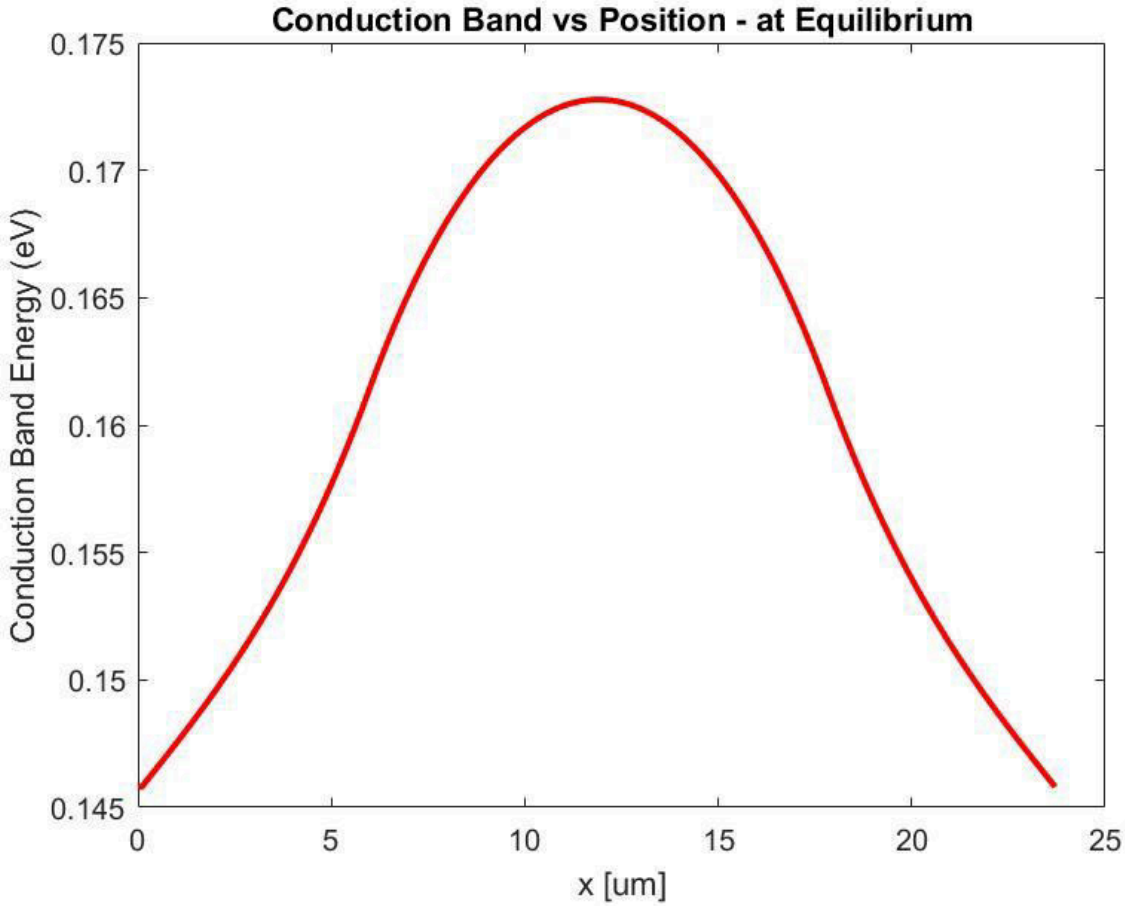

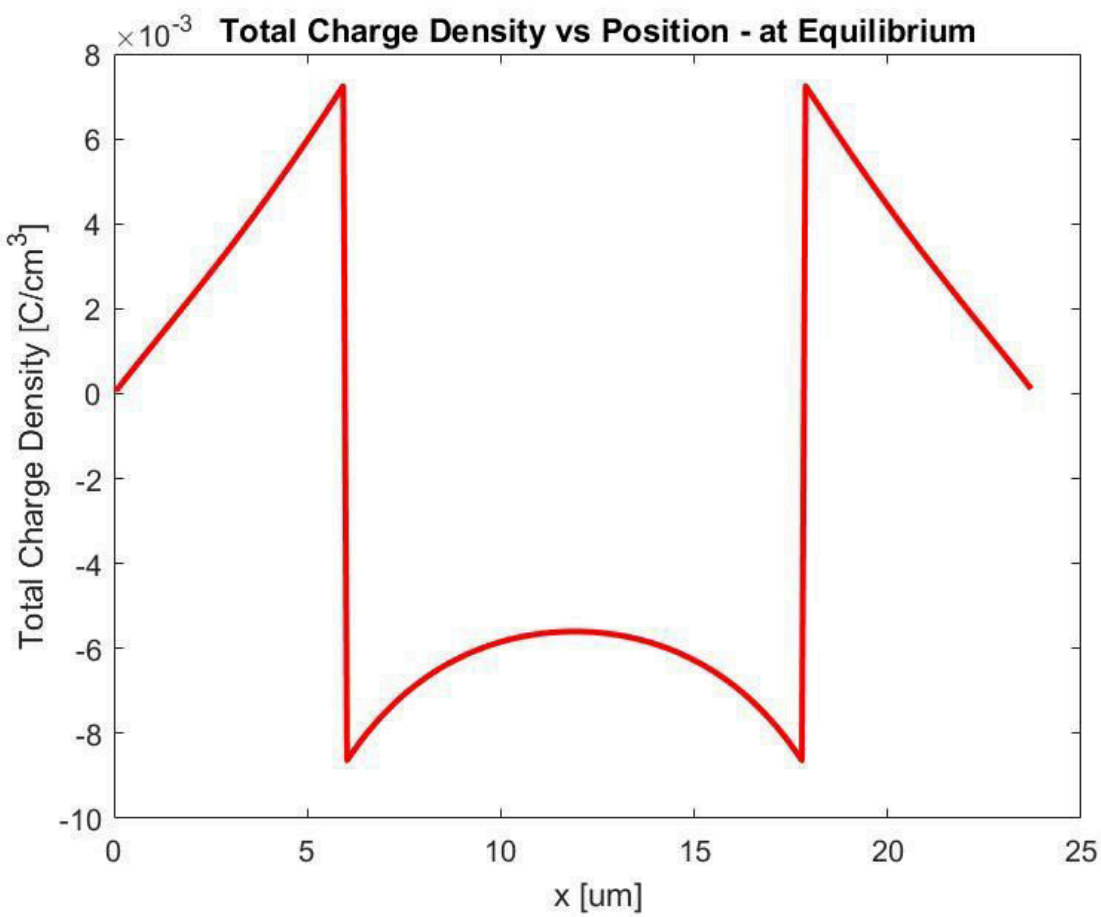

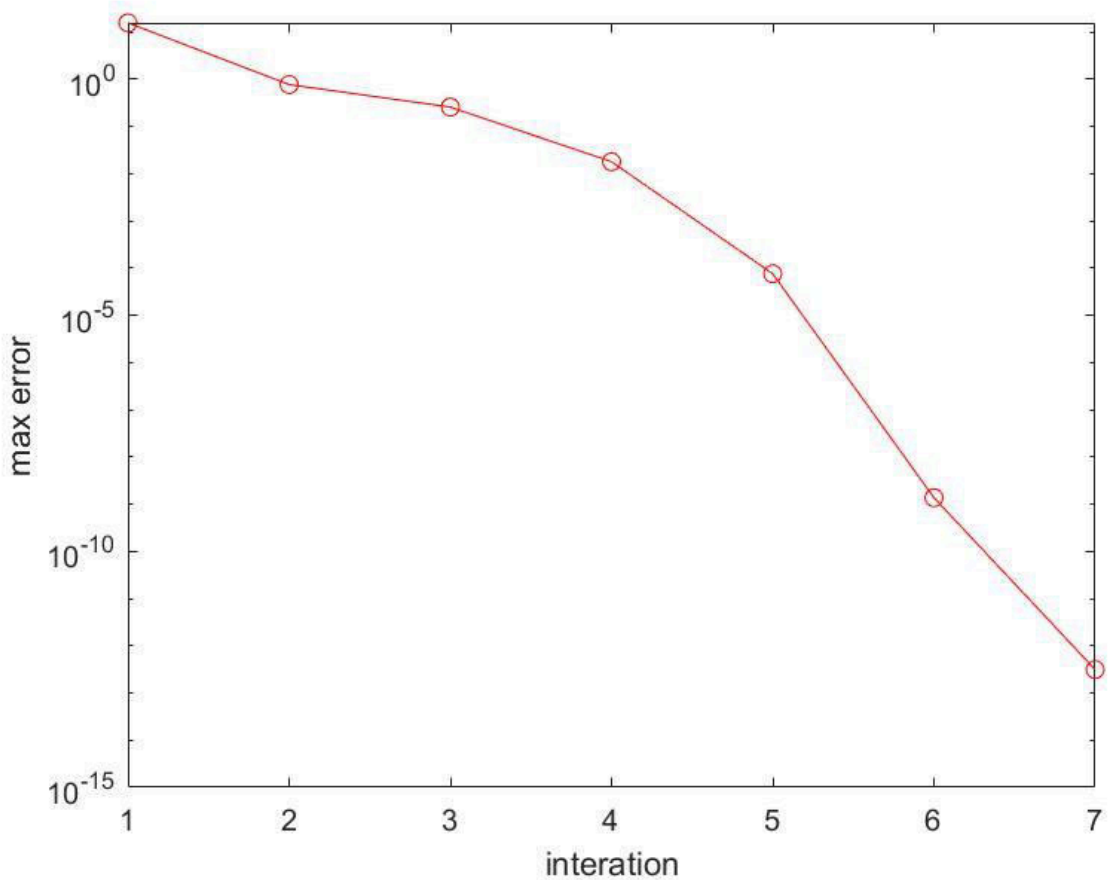
max error
interation
10^{0}
10^{-5}
10^{-10}
10^{-15}
1
2
3
4
5
6
7

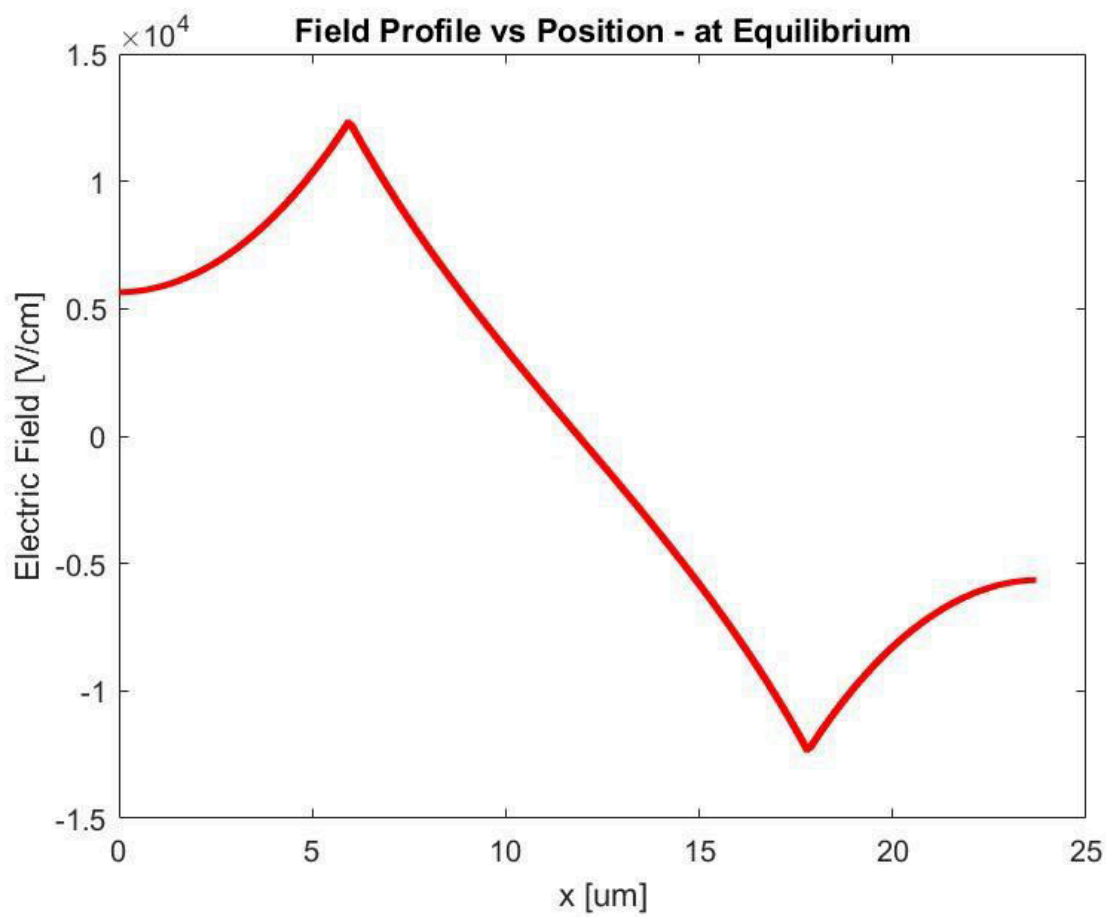
Field Profile vs Position - at Equilibrium
$\times 10^{4}$
Electric Field [V/cm]
x [um]
1.5
1
0.5
0
-0.5
-1
-1.5
0
5
10
15
20
25

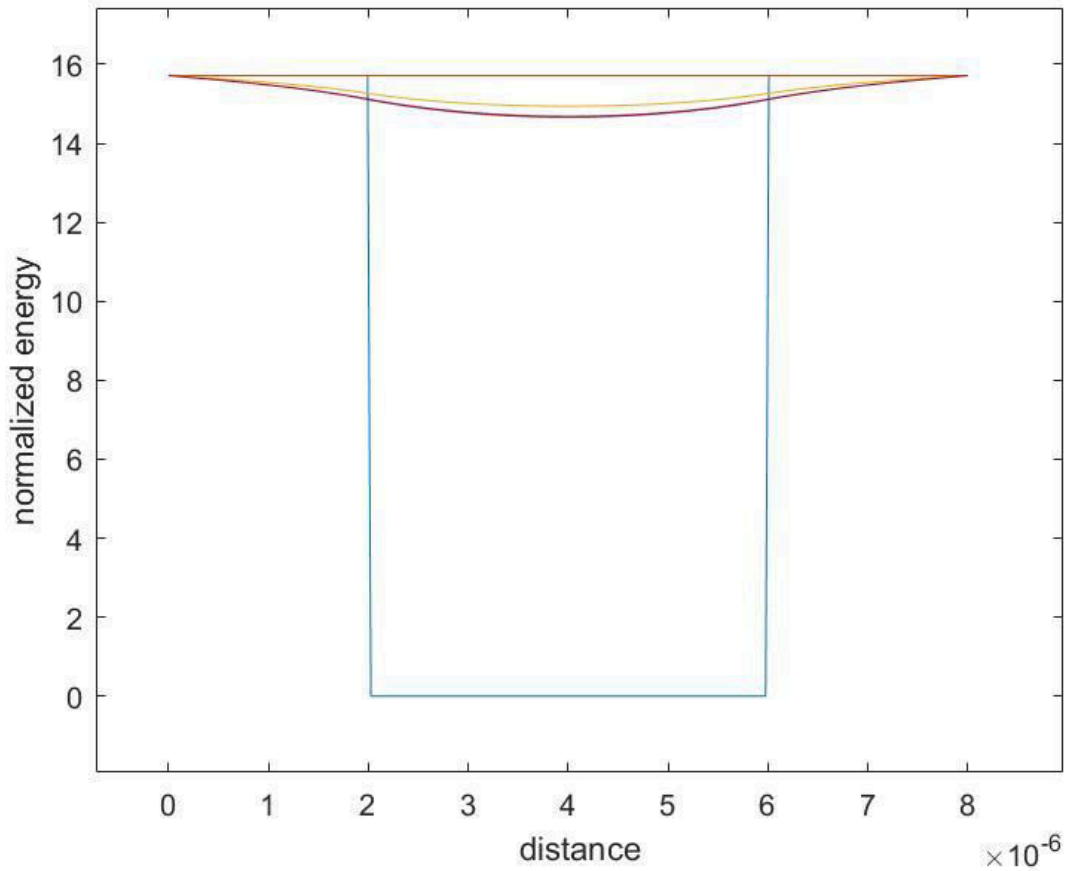
normalized energy
distance
×10^-6
0
1
2
3
4
5
6
7
8
0
2
4
6
8
10
12
14
16

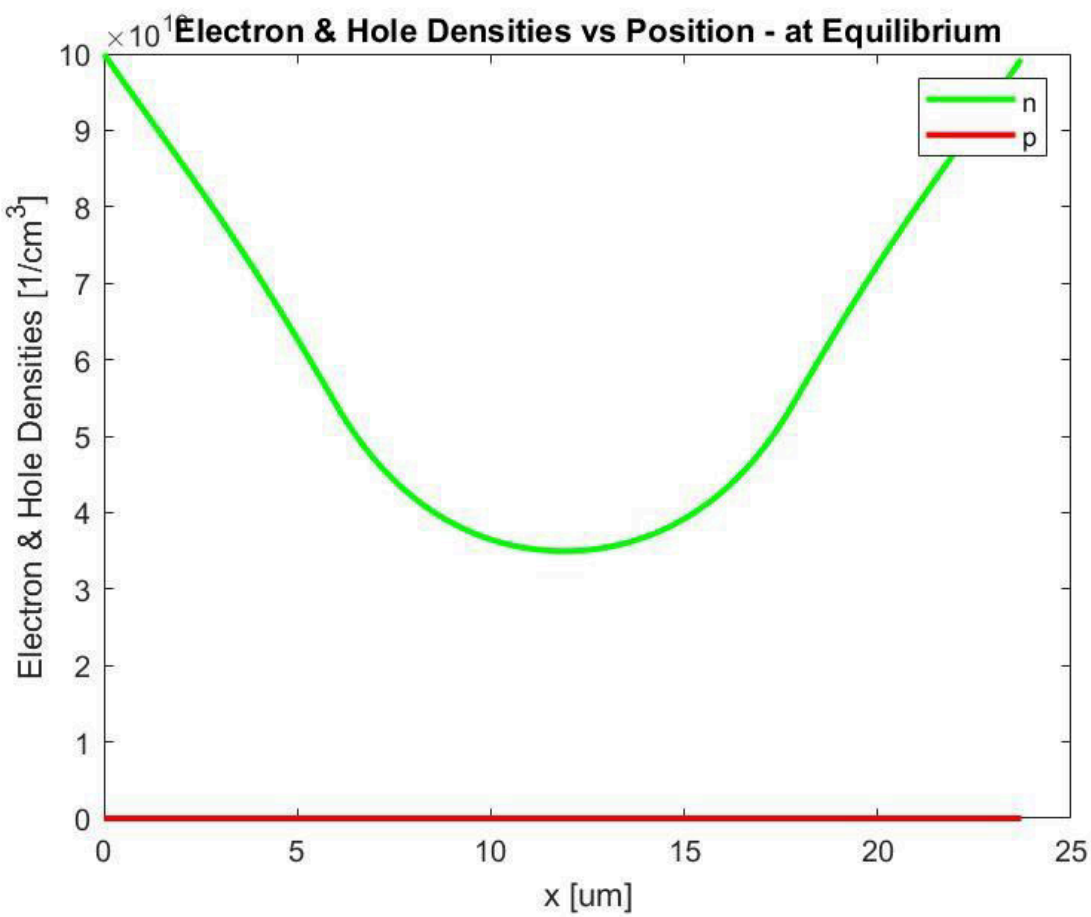
Electron & Hole Densities vs Position - at Equilibrium
×10^16
Electron & Hole Densities [1/cm^3]
x [um]
n
p
0
5
10
15
20
25
0
1
2
3
4
5
6
7
8
9
10

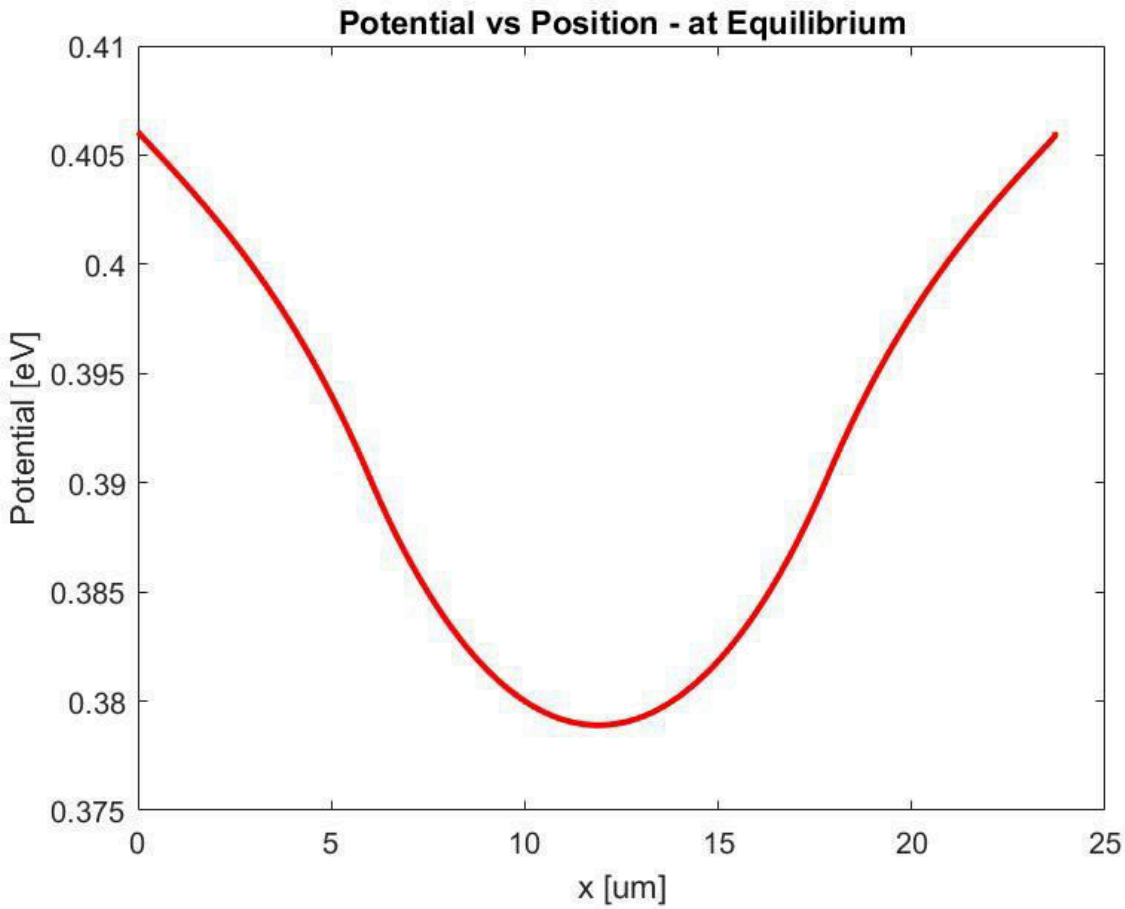

The plots match the expected profiles as we derived in class, the only difference being that we used the depletion approximation to get perfectly rectangular profiles in class. In contrast, here, a more realistic calculation shows the rectangles are not perfectly flat but slightly bent, which was expected because of the exponential terms in the Poisson equation.

Variation of barrier height with doping for NIN

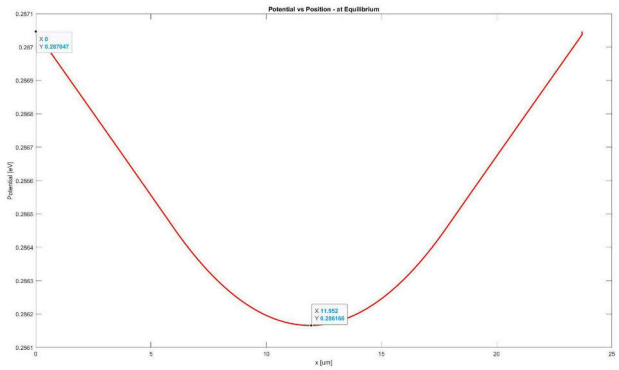

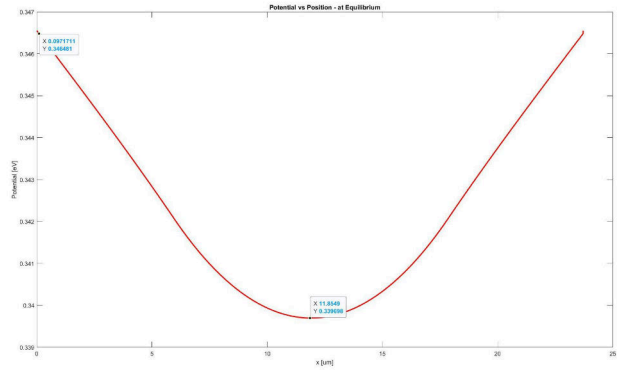

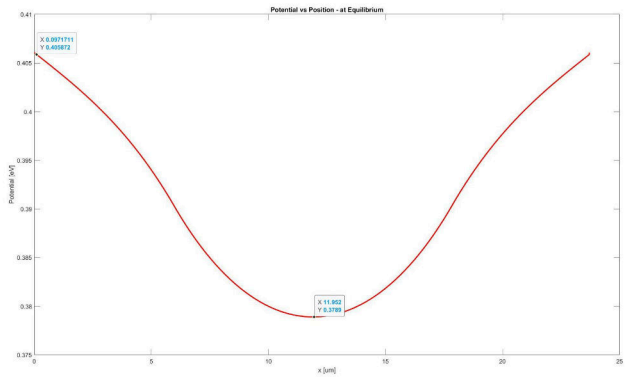

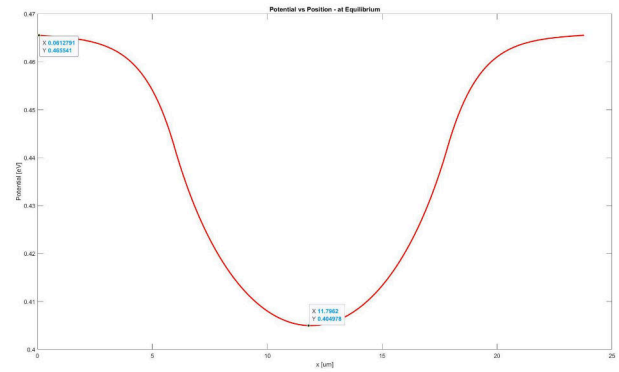

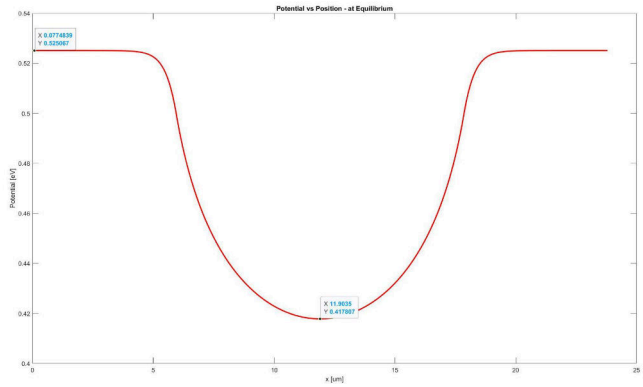

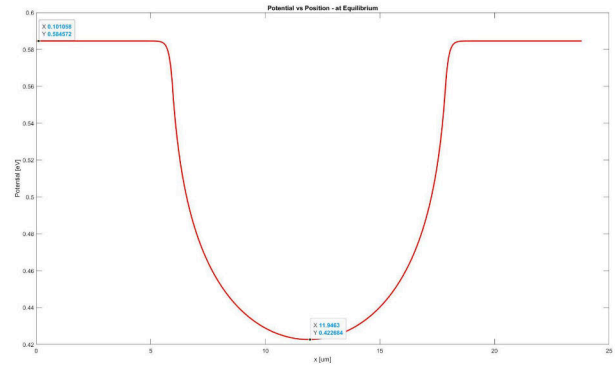

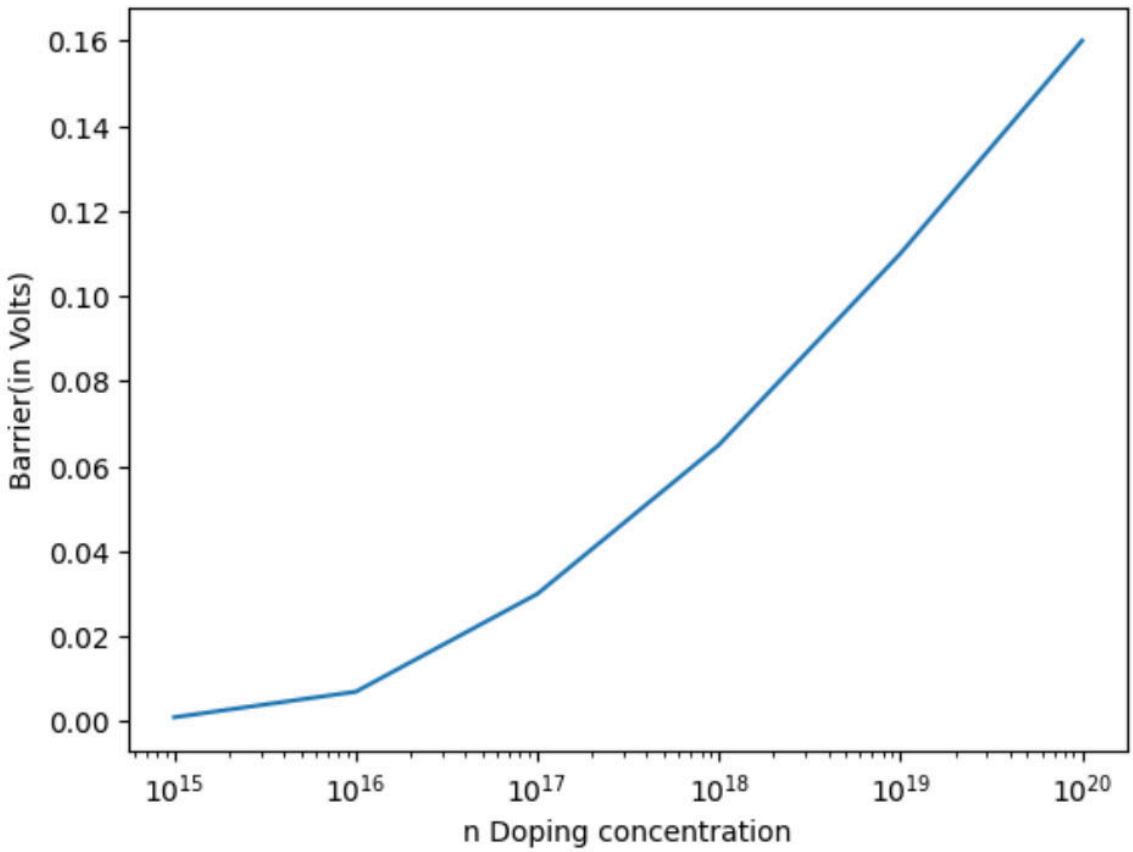

Increasing the n-type dopant concentration in a p-n junction initially elevates the built-in potential and barrier height due to enhanced Fermi level separation. However, this effect eventually saturates at high doping levels, where electron-electron repulsion limits further Fermi-level advancement.

Answer 4

4.

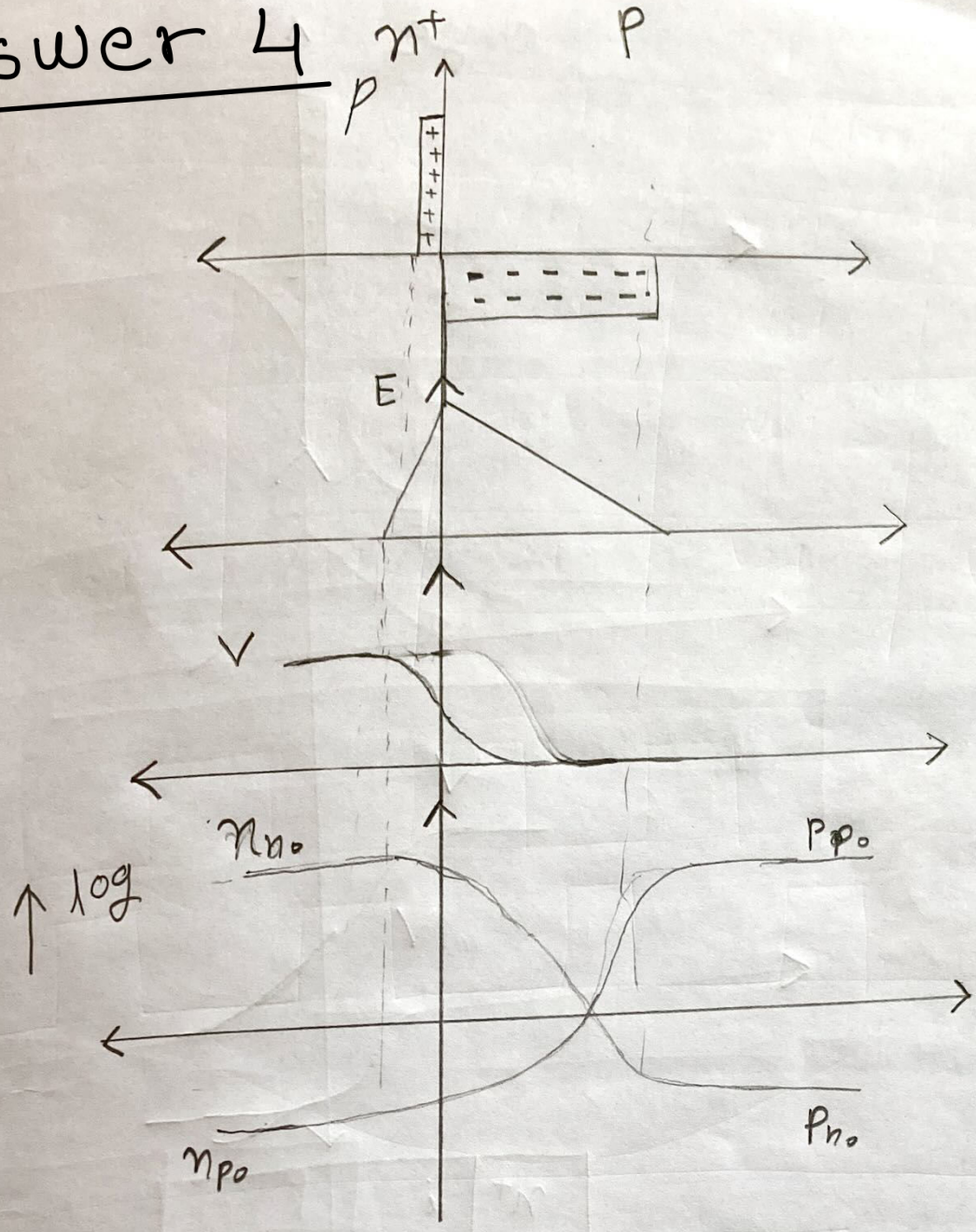

For $n^+ (10^{20}/cc)$ and $P(10^{18}/cc)$

Due to its n^+-p structure we can use the formulae

$$\psi_{bi} = \frac{E_g}{2q} + \frac{KT}{q} \ln(N_a/n_i)$$

$$\frac{1.1}{2} + 25\times10^{-3} \ln\left(\frac{N_a}{10^{10}}\right) = 0.6$$

$$25\times10^{-3} \ln(N_a/10^{10}) = 0.05$$

$$\ln(N_a/10^{10}) = \frac{0.05}{25}\times10^{3} =$$

$$N_a = 7.38\times10^{10}\ cm^{-3}$$

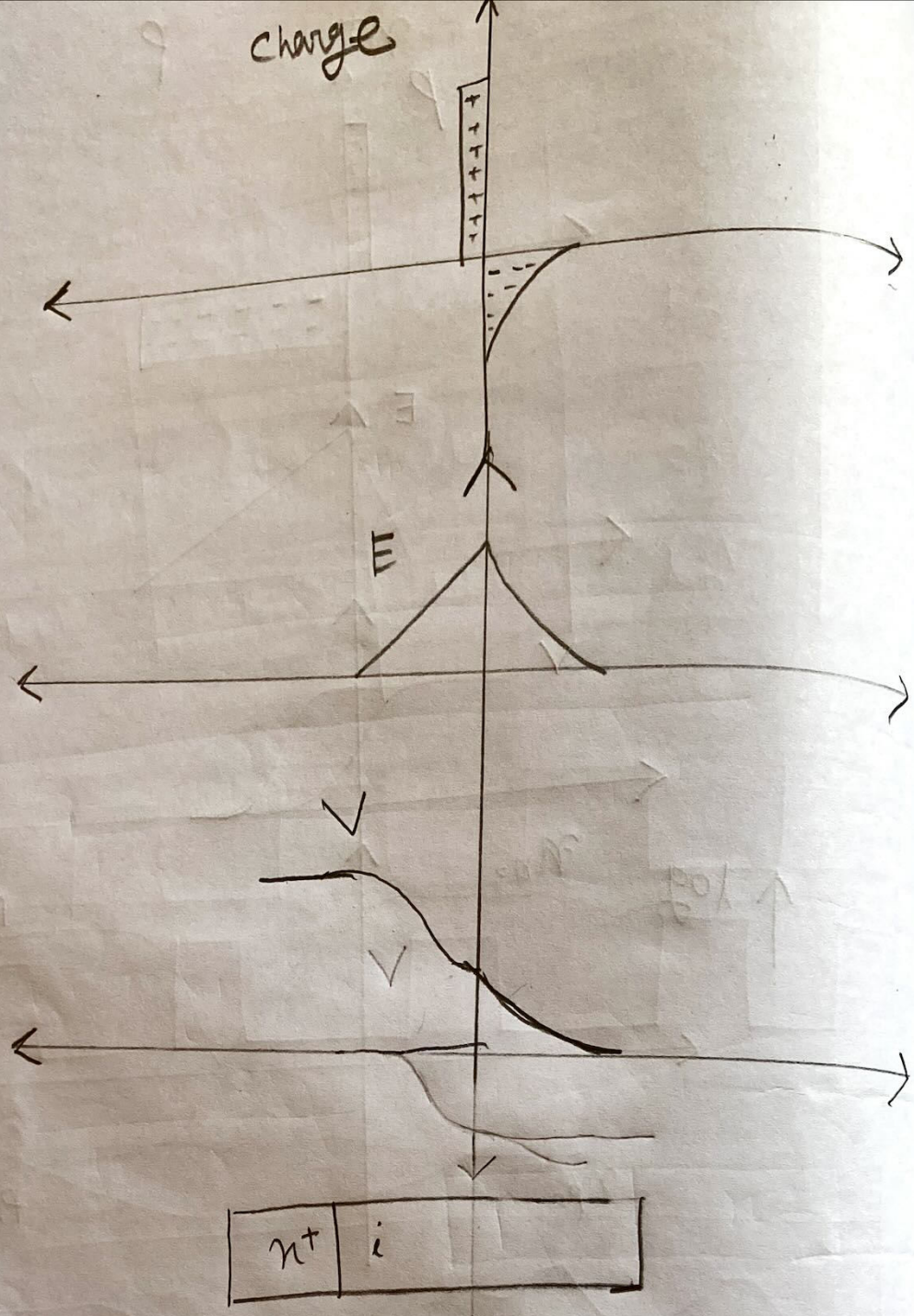
charge
E
V
n+
i

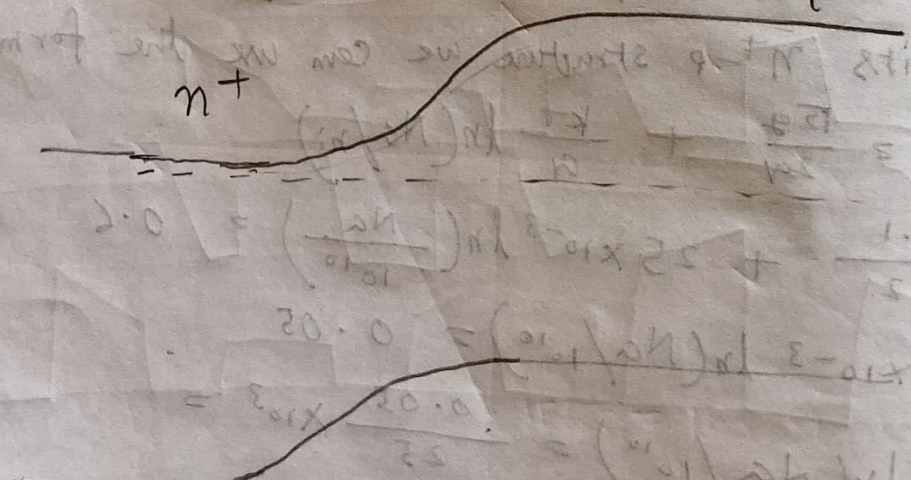
i
n+

4. (b) Without changing doping if we can use different material for -i region then we can change barrier height to 0.5v.

Analytical Solution :-

$$\frac{d^2V(x)}{dx^2} = -\frac{q}{\epsilon} N_D^+ \quad \text{For } n^+ \text{ region}$$

$$\frac{d^2V(x)}{dx^2} = \frac{-q}{\epsilon} n_i e^{\frac{qV(x)}{KT}} \quad \text{For intrinsic region}$$

so for V(x) in n^+ region it will be parabolic potential.

For ~~at~~ intrinsic region ~~it is~~ we can approx.

$$e^{\frac{qV(x)}{KT}} = 1 + \frac{qV(x)}{KT}$$

$$\frac{d^2V(x)}{dx^2} = -\frac{q}{\epsilon} n_i \left[1 + \frac{qV(x)}{KT}\right]$$

So, we can ~~we~~ get exponential decay solution of potential.

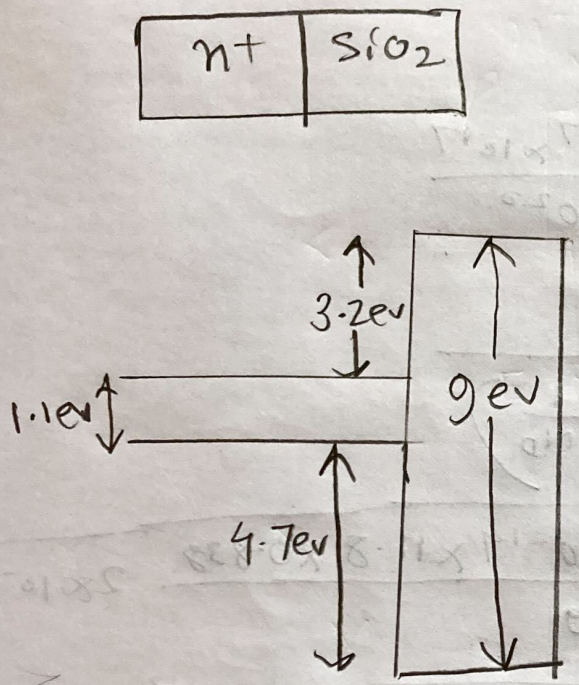

As SiO_2 is a insulator it will prevent charge transfer.

Answer 5

Q.5

(a)

$$V_{bi} = V_T \ln \frac{N_A N_D}{n_i^2}$$

$$= 26\,mV \times \ln \frac{10^{17} \times 10^{17}}{10^{20}}$$

$$= 0.838\ V$$

$$W = \sqrt{\frac{2\epsilon V_{bi}}{q}\left(\frac{1}{N_A} + \frac{1}{N_D}\right)}$$

$$= \sqrt{\frac{2 \times 8.854 \times 10^{-14} \times 11.8 \times 0.838}{1.6 \times 10^{-19}} \cdot 2 \times 10^{-17}}\ cm$$

$$= \sqrt{\frac{4 \times 8.854 \times 11.8 \times 0.838}{1.6} \times 10^{-12}}\ cm$$

$$= 14.78 \times 10^{-8}\ m$$

$$|E_{max}| = \frac{2 \times 0.838}{14.78 \times 10^{-8}} = 11.33 \times 10^{6}\ V/m$$

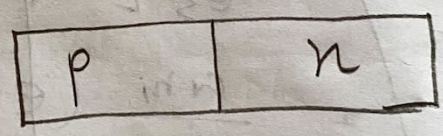

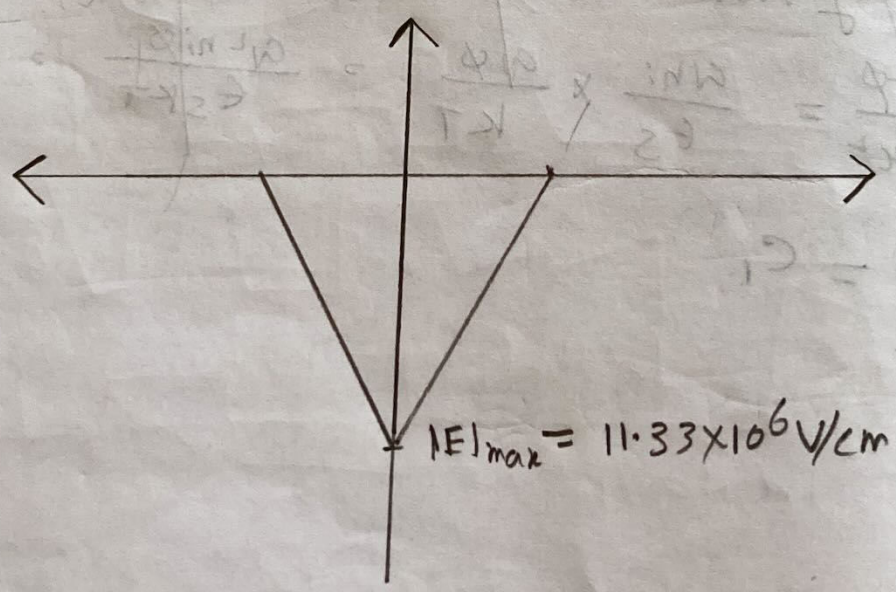

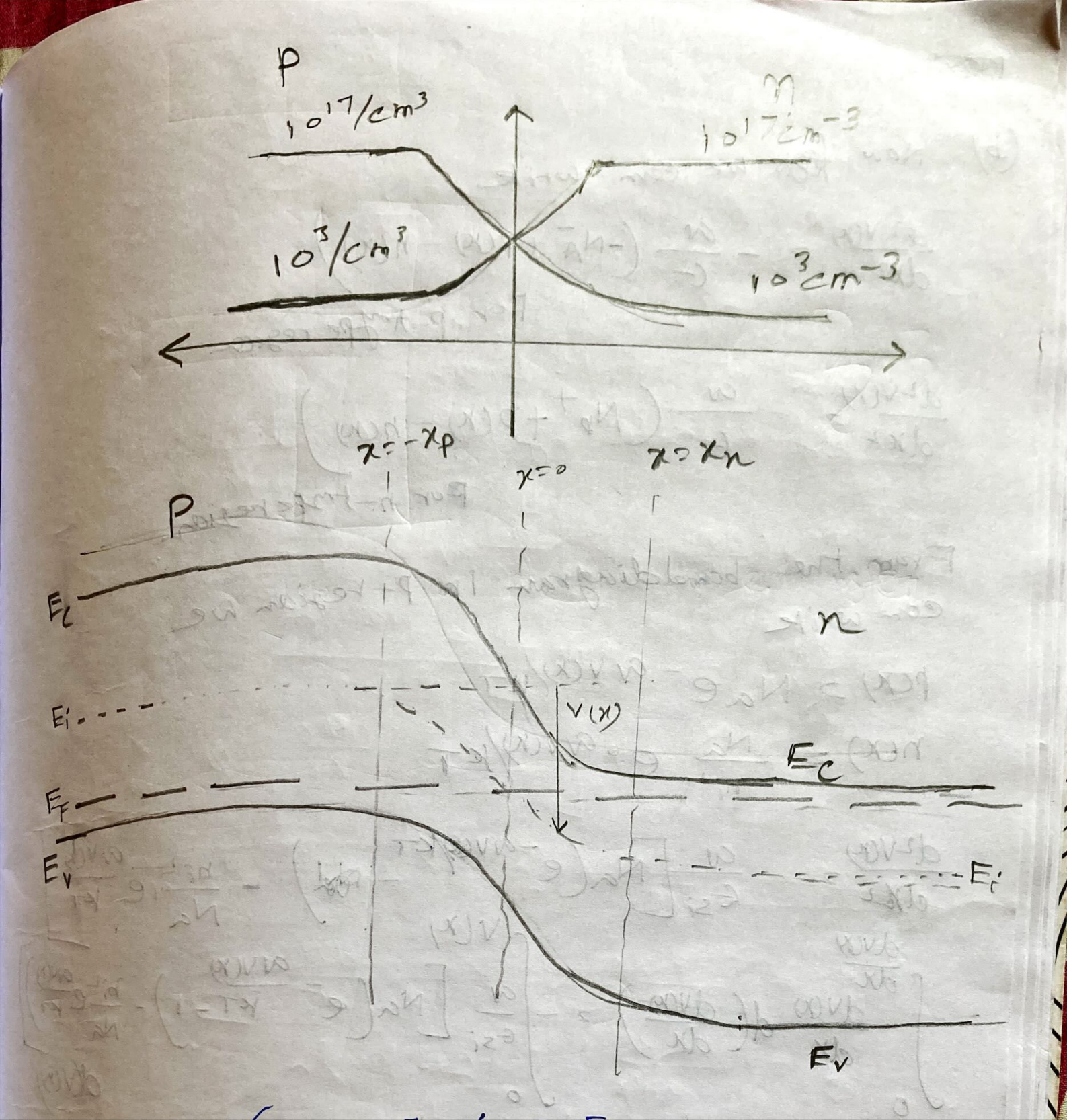
p
$10^{17}/cm^3$
n
$10^{17} cm^{-3}$
$10^3/cm^3$
$10^3 cm^{-3}$
$x = -x_p$
$x = 0$
$x = x_n$
p
n
E_c
E_i
$V(x)$
E_c
E_F
E_v
E_i
E_v

(b) Now we can write

$$\frac{d^2V(x)}{dx^2} = -\frac{q}{\epsilon}\left(-N_A^- + p(x) - n(x)\right)$$

For p-type region

$$\frac{d^2V(x)}{dx^2} = -\frac{q}{\epsilon}\left(N_D^+ + p(x) - n(x)\right)$$

For n-type region

From the band diagram in p-region we can write

$$p(x) = N_a e^{-qV(x)/kT}$$

$$n(x) = \frac{N_a}{n_i^2} e^{qV(x)/kT}$$

$$\frac{d^2V(x)}{dx^2} = -\frac{q}{\epsilon_{si}}\left[N_a\left(e^{-qV(x)/kT} - 1\right) - \frac{n_i^2}{N_a} e^{\frac{qV(x)}{kT}}\right]$$

$$\int_0^{\frac{dV(x)}{dx}} \frac{dV(x)}{dx}\, d\left(\frac{dV(x)}{dx}\right) = -\int_0^{V(x)} \frac{q}{\epsilon_{si}}\left[N_a\left(e^{-\frac{qV(x)}{kT}} - 1\right) - \frac{n_i^2}{N_a} e^{\frac{qV(x)}{kT}}\right] d(V(x))$$

$$\frac{1}{2}\left[\frac{dV(x)}{dx}\right]^2 = \frac{2kTN_a}{\epsilon_{si}}\left[\left(e^{-\frac{qV(x)}{kT}} + \frac{qV}{kT} - 1\right) + \frac{n_i^2}{N_a}\left(e^{\frac{qV(x)}{kT}} - \frac{qV}{kT} - 1\right)\right]$$

5.(b)

p	n

Including the dominating free carrier term

$$\rho = q\left(p(x) - n(x) + N_D^+(x) - N_A^-(x)\right)$$

$$\frac{d^2V(x)}{dx^2} = -\frac{q}{\epsilon_{Si}}\left[p(x) - n(x) + N_D^+(x) - N_A^-(x)\right]$$

for p side $p(x)$ will be the dominated term
n side $n(x)$ will be the dominated term

(c) so $V(x)$ is the potential $\psi(x=-\alpha)=0$ as reference,
analysis for the p-side $(-\alpha < x \le 0)$

$$p(x) = n_i e^{\frac{E_i(x) - E_F}{kT}}$$

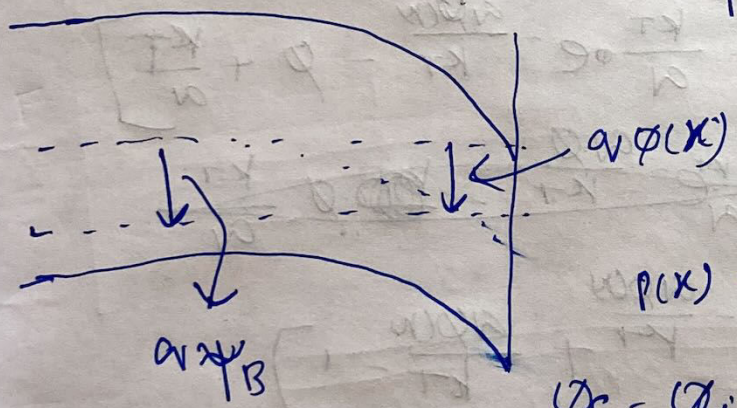

$$\phi(x) = \phi_i(x)$$

$$\phi_B = \phi_f$$

$$p(x) = n_i e^{\frac{q(\phi_f - \phi_i(x))}{kT}}$$

$$\phi_f - \phi_i(x) = \phi_B(x) - \phi(x)$$

$$p(x) = n_i e^{\frac{q(\phi_B - \phi(x))}{kT}}$$

say
$$p_0 = p(x=-\alpha) = n_i e^{\frac{q\phi_B}{kT}}$$
$$= N_A e^{-\frac{q\phi(x)}{kT}}$$

Poisson equation for p-side

$$\frac{d^2V(x)}{dx^2} = \frac{-q}{\epsilon_{Si}}\left[N_A e^{-\frac{q\phi(x)}{kT}} - N_A\right]$$

$N_D \rightarrow$ Ignoring
$n(x) \rightarrow$ guided to take dominated term

$$\frac{d^2\phi}{dx^2} = -\frac{q}{\epsilon_{si}} N_A \left[e^{-\frac{q\phi(x)}{KT}} - 1 \right]$$

In Bulk $(x = -\infty)$ $\varphi = 0$, $\frac{d\varphi}{dx} = 0$ also

E at $(x = -\infty)$ will be 0 since potential is also vanishing at infinite length.

Multiply both side by $\left(\frac{d\phi}{dx}\right) dx$ and integrating form bulk to surface

$$\int_0^{\frac{dv}{dx}} \frac{d\phi(x)}{dx} d\left(\frac{d\phi}{dx}\right) = -\int_0^{L} \frac{q}{\epsilon_{si}} N_A \left[e^{-\frac{q\phi(x)}{KT}} - 1 \right] d\phi$$

$$\frac{1}{2}\left(\frac{d\phi}{dx}\right)^2 = -\frac{qN_A}{\epsilon_{si}} \left[\frac{e^{-q\phi(x)/KT}}{-q/KT} - \phi \right]_0^{\phi}$$

$$= \frac{-qN_A}{\epsilon_{si}} \left[-\frac{KT}{q} e^{-\frac{q\phi(x)}{KT}} - \phi + \frac{KT}{q} \right]$$

$$\cancel{[E(x)]^2 = \frac{2KTN_A}{\epsilon_{si}} \left[\frac{KT}{q} e^{-\frac{q\phi}{KT}} - \phi - \frac{KT}{q} \right]}$$

$$[E(x)]^2 = \frac{2KTN_A}{\epsilon_{si}} \left[e^{-\frac{q\phi(x)}{KT}} + \frac{q\phi(x)}{KT} - 1 \right]$$

$$L_D^2 = \frac{\epsilon_{si} KT}{qN_A} \quad \text{Debye length}$$

$$E(x) = -\sqrt{2}\, q \frac{N_D L_D}{\epsilon_{si}} \left(e^{-\frac{\phi}{V_T}} + \frac{\phi}{V_T} - 1 \right)^{1/2}$$

when $\phi > 0$ and $|\phi/V_T| \gg 0$

(Here we have only calculated p side)

$$E(x) = -\sqrt{2}\, q \frac{N_A L_D}{\epsilon_{Si}} \sqrt{\frac{\phi}{V_T}}$$

$$= -\sqrt{\frac{2 q N_A \phi}{\epsilon_{Si}}}$$

Because ϕ is shown downward in the diagram potential is negative for $\phi > 0$.

So we find $V \propto x^2$ and $E \propto x$

That means depletion approx. valid.

For $\phi < 0$ and $|\phi/V_T| \sim 0$ for p-side

$$E(x) = -\sqrt{2q} \frac{N_A L_D}{\epsilon_{Si}} \left(e^{-\frac{\phi}{V_T}} + \frac{\phi}{V_T} - 1 \right)^{1/2}$$

$$= -\sqrt{2q} \frac{N_A L_D}{\epsilon_{Si}} e^{-\frac{\phi}{2V_T}}$$

$$\frac{d\phi}{dx} = \pm \sqrt{\frac{2KTN_A}{\epsilon_{Si}}} \left[e^{-\frac{\phi}{V_T}} + \frac{\phi}{V_T} - 1 \right]^{1/2}$$

Solving this equation analytical is looking very difficult.

We have to solve it numerically.

$$\frac{d^2\phi}{dx^2} = -\frac{q}{\epsilon_{Si}} N_A \left[e^{-\frac{q\phi(x)}{KT}} - 1 \right]$$

Discritize the ϕ in no of mesh in space.

solve via Newton Raphson method for n variable using matrices

$$f = A * psi - b$$

$A \rightarrow$ tridiagonal matrix, $b =$ RHS of above equation

Now Jacobian will be done

We will iterate several time as we do in newton raphson

$$\frac{2KTN_A}{\epsilon_{si}} = 2\left(\frac{V_T}{L_D}\right)^2 = \frac{2q^2 N_A^2 L_D^2}{\epsilon_{si}}$$

(d) $$E(x) = -\sqrt{2}\,\frac{V_T}{L_D}\left(e^{-\frac{\phi}{V_T}} - \frac{\phi}{V_T} - 1\right)^{1/2}$$

$$C = \left|\frac{d\phi}{dV_a}\right| = \epsilon_s\left|\frac{dE}{d\phi}\right|$$

$$= \left|-\frac{\sqrt{2}V_T\epsilon_s}{L_D V_T} \times \frac{-e^{-\phi(x)/V_T} - 1}{2\sqrt{e^{-\phi(x)/V_T} - \frac{\phi(x)}{V_T} - 1}}\right|$$

$$= \left|\frac{\epsilon_s}{L_D}\,\frac{e^{-\phi(x)/V_T} + 1}{\sqrt{2\left(e^{-\phi(x)/V_T} - \frac{\phi(x)}{V_T} - 1\right)}}\right|$$

The difference may be done to the p-side solution if I had take n-side solution then I would have neglected other two term in the poisson equation with the dominated free carrier and also it may be done to my connection on taking downward bending as ϕ.

(e) ϕ_s potential across semiconductor depletion $= V_{bi}$

$= -\phi_i + V_a$

$\phi_s > 0$ and $|\phi_s| \gg V_T \Rightarrow e^{-\phi/V_T} \ll 1$

$$C = \frac{\epsilon_s}{L_D} \frac{1}{\sqrt{2\left[-\left(\frac{-\phi_s + V_a}{V_T}\right) - 1\right]}}$$

$$= \frac{\epsilon_s}{L_D} \sqrt{\frac{V_T}{2(\phi_s - V_a - V_T)}} \quad \because \sqrt{V_T} = L_D \sqrt{qN_A/\epsilon_{si}}$$

$$= \sqrt{\frac{\epsilon_s q N_A}{2|\phi_i - V_a - V_T|}}$$

with full depletion approx. we had gotten

$$E(x) = -\sqrt{\frac{2qN_A\phi}{\epsilon_{si}}}$$

$$C = \epsilon_{si}\left|\frac{dE}{d\phi}\right| = \sqrt{\frac{qN_A\epsilon_{si}}{2\phi}} = \sqrt{\frac{qN_A\epsilon_{si}}{2|\phi_i - V_n|}}$$

Q.2

a.

E(k) = Eo + (h/2pi)^2 k^2 / 2m*

Where m* = 0.5mo

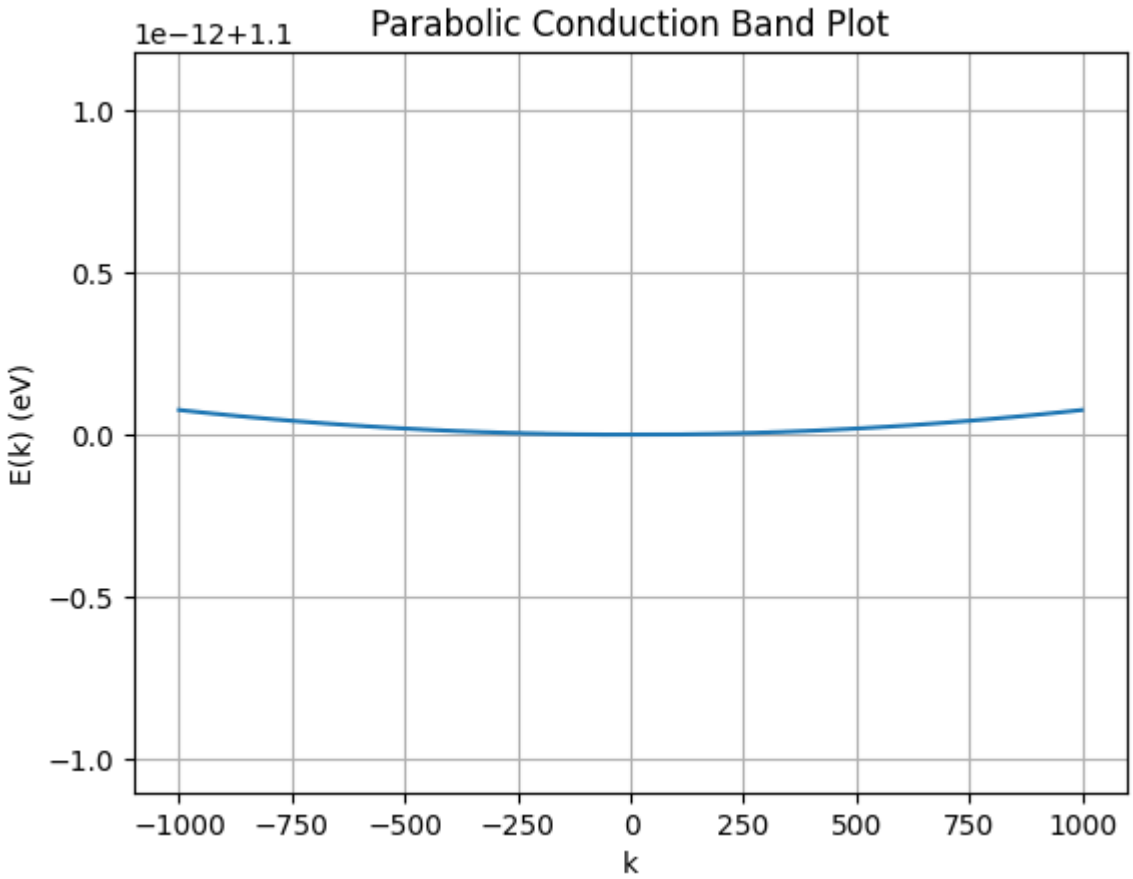

Note: y-axis has an offset of 1.1 (eV) added.

b. **Carrier Statistics:**

$$f(E) = \frac{1}{1 + e^{(E-E_F)/kT}} \qquad f_{\mathrm{MB}}(E) = e^{-(E-E_F)/kT}$$

I tried the exercise on MATLAB, but was constantly getting plots with unreasonable values. So, I did the same in python. Following are the plots:

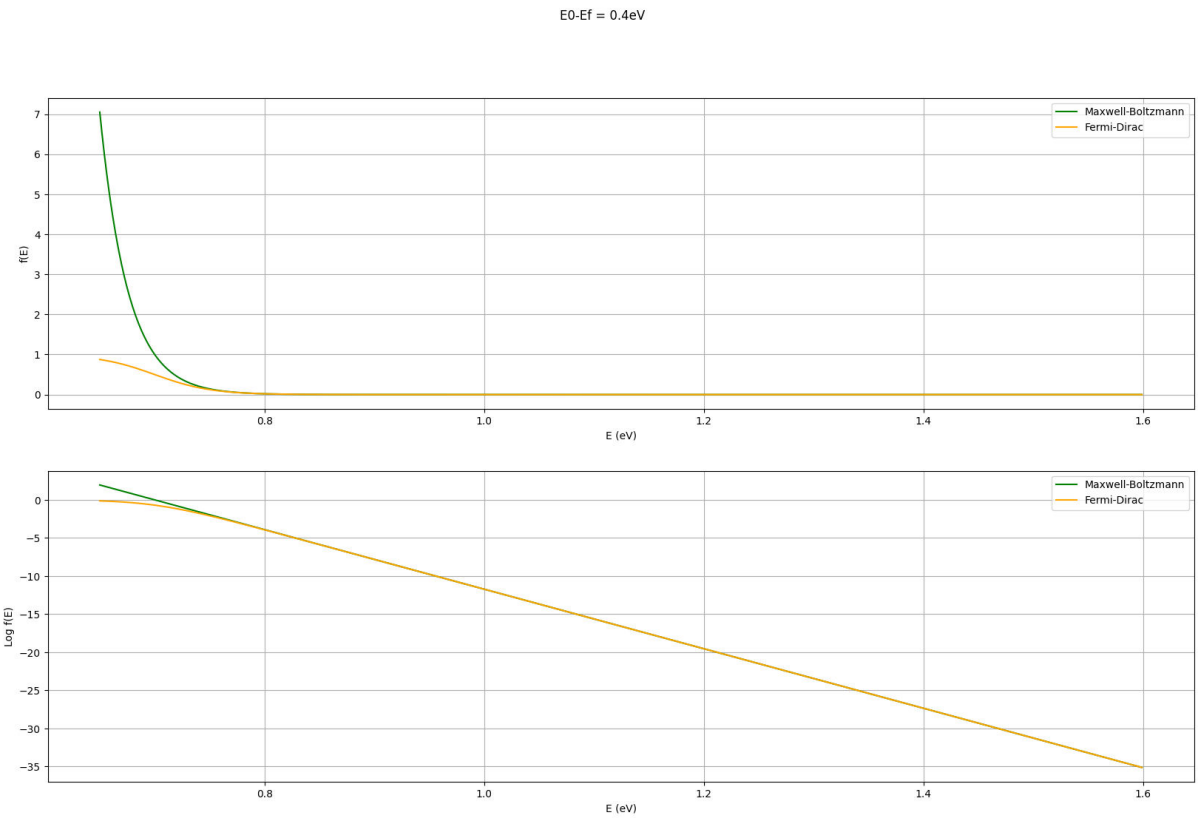

c. I numerically integrated the expression:

$$n = \int_{E_c}^{\infty} g_c(E) f(E) dE = \frac{(m_n^*)^{3/2}\sqrt{2}}{\pi^2 \hbar^3} \int_{E_c}^{\infty} \frac{\sqrt{E - E_c}}{1 + e^{(E - E_F)/kT}} dE$$

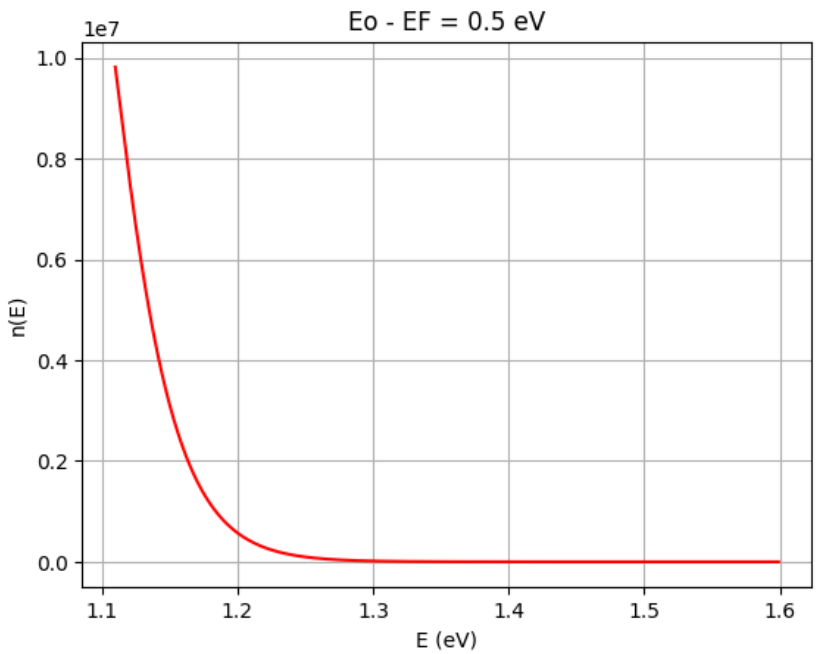

d. Repeating parts b and c for Eo – EF = 0.05 eV,

b.

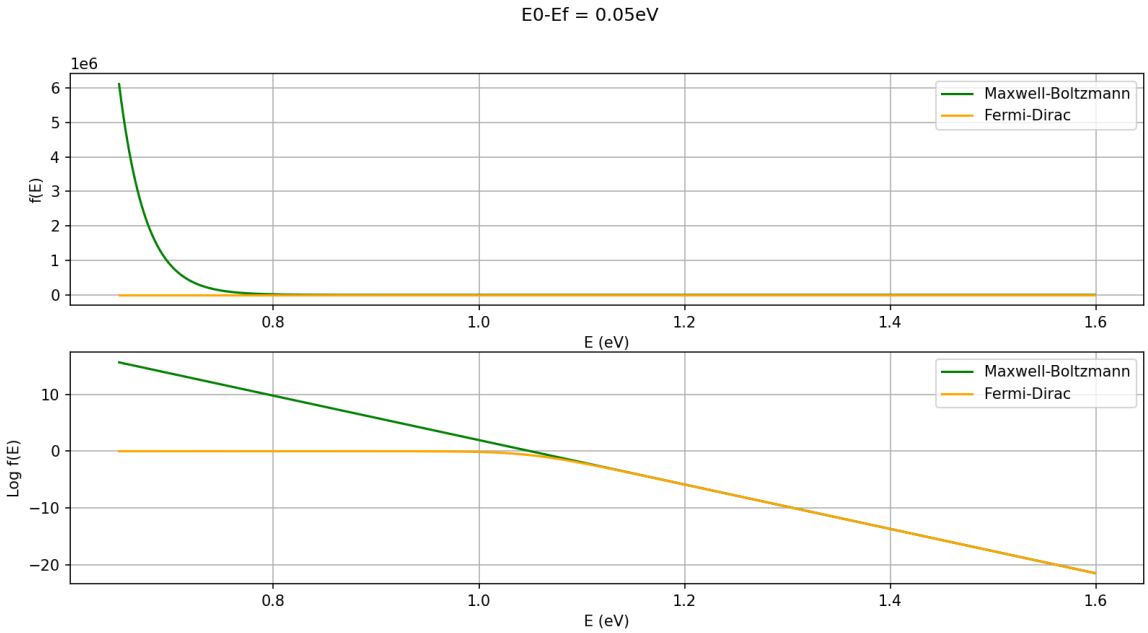

c.

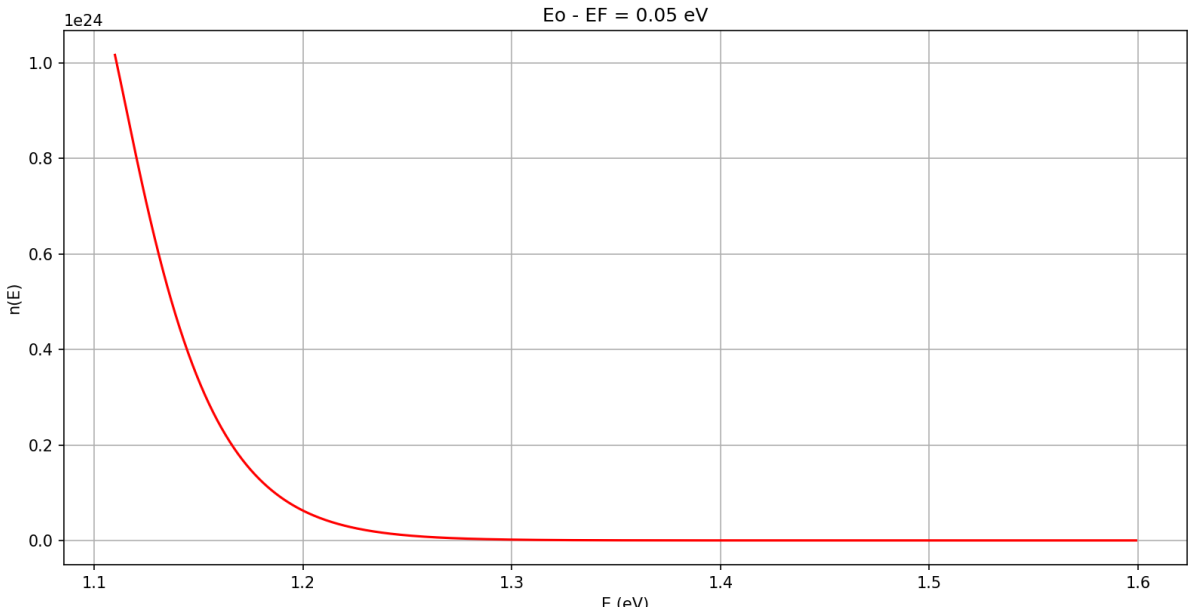

e. Plots:

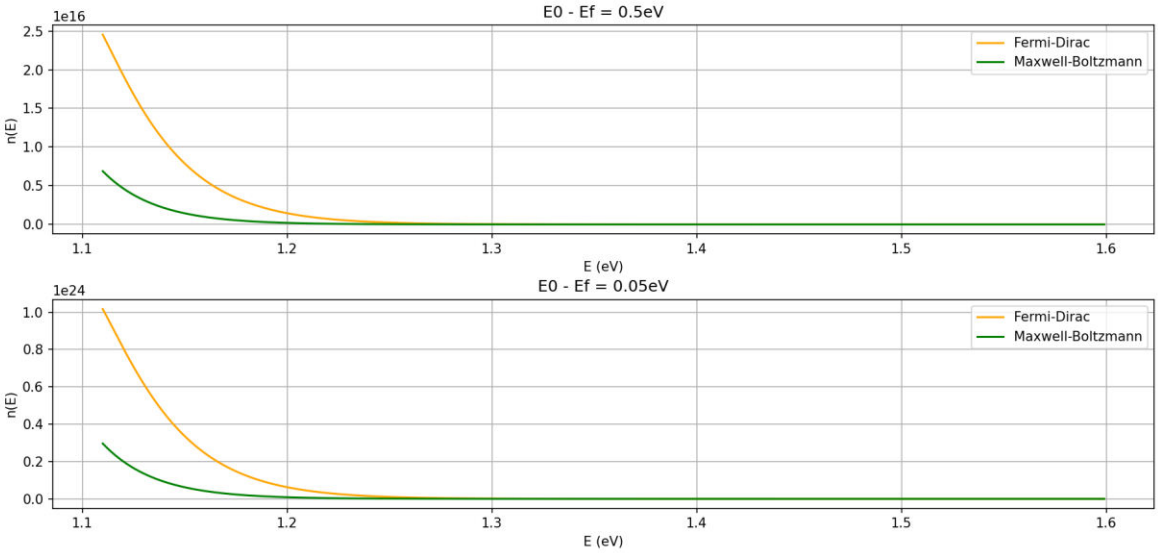

As seen from above plots, as energy increases, the values computed by both methods agree. This is because of the assumption $e^{(E-E_F)/kT} \gg 1$, which becomes more and more valid. At lower values though, deviation is observed since assumption is invalid.

Another observation is, that for both values of E0 – EF, the both methods agree over the same range of E. This is because the approximation only depends on E-EF and not on E0.

Q.3

Q.3 Let depletion width be $2W$. $\rho(x) = Nx$ where $N = 10^{23}\ cm^{-4}$.

Depletion approximation:

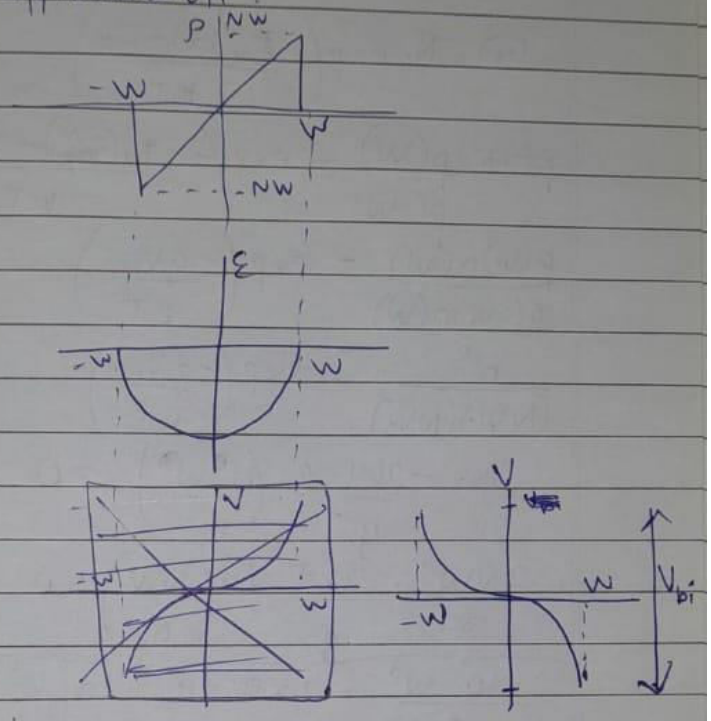

$$\rho(x) = Nx$$

$$\mathcal{E}(x) = \frac{1}{\epsilon}\int_{-W}^{x}(Nx)\,dx + c_0$$

$$= \frac{N}{2\epsilon}(x^2 - W^2) + 0$$ ... (boundary condition: $\mathcal{E} = 0$ outside depletion region)

$$V(x) = -\int \frac{N}{2\epsilon}(x^2 - W^2)\,dx + c_1$$

$$= \frac{N}{2\epsilon}\left(W^2 x - \frac{x^3}{3}\right) + c_1$$

$$V(W) - V(-W) = \frac{N}{2\epsilon}\left(W^3 - \frac{W^3}{3}\right) - \frac{N}{2}\left(-W^3 + \frac{W^3}{3}\right)$$

$$\therefore V_{bi} = \frac{2NW^3}{3\epsilon}$$

built in voltage

PAGE No.
DATE / /

Now, we will use carrier statistics:

$$p(x) = N_v \exp\left(-\frac{E_F - E_v(x)}{kT}\right)$$

$$n(x) = N_c \exp\left(-\frac{E_c(x) - E_F}{kT}\right)$$

$$\frac{p(W)}{p(-W)} = \exp\left(-\frac{E_v(-W) - E_v(W)}{kT}\right)$$

$$\frac{p(W)n(W)}{p(-W)n(W)} = \exp\left(-\frac{qV_{bi}}{kT}\right)$$

$$\frac{n_i^2}{(NW)(NW)} = \exp\left(-\frac{qV_{bi}}{kT}\right)$$

$$V_{bi} - \frac{2kT}{q}\ln\left(\frac{N^2W^2}{n_i}\right) = 0$$

$$\frac{2NW^3}{3\epsilon} - \frac{2kT}{q}\ln\left(\frac{NW}{n_i}\right) = 0$$

$$\frac{2\times10^{23}W^3}{2\times11.7\times8.85\times10^{-12}} - 2\times26\times10^{-3}\ln\left(\frac{10^{23}W}{10^{10}}\right) = 0$$

Solving using DESMOS, $W = 7 \times 10^{-12}$

~~$W = 10^{-11}$ m = 10 pm~~

Since we had assumed depletion, we now proceed to calculate free carriers (inaccurate in 1st iteration):

On the p-side:

$$p - n - N_a = 0$$

$$p - \frac{n_i^2}{p} + Nx = 0$$

$$p^2 + Nxp - n_i^2 = 0$$

$$\therefore p = \frac{\sqrt{N^2x^2 + 4n_i^2} - Nx}{2}$$

$$\therefore n = \frac{2n_i^2}{\sqrt{N^2x^2 + 4n_i^2} - Nx}$$

Observing the plots, n is insignificant compared to p to compute voltage error.

On the n-side, similarly,

$$\frac{n_i^2}{n} - n + Nx = 0$$

$$\therefore n = \frac{\sqrt{N^2x^2 + 4n_i^2} \quad Nx}{2} \quad \text{and}$$

$$p = \frac{2n_i^2}{\sqrt{N^2x^2 + 4n_i^2} \quad Nx}$$

Finding solution of equation using DESMOS:

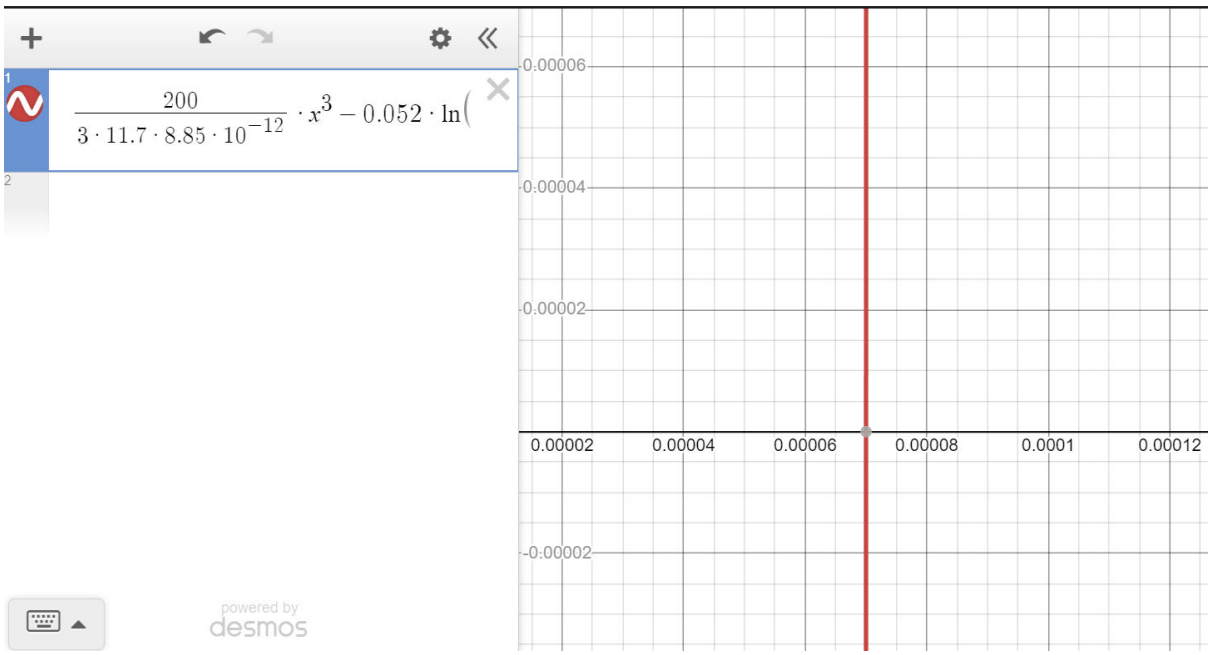

Free Carrier Concentration in the Depletion region:

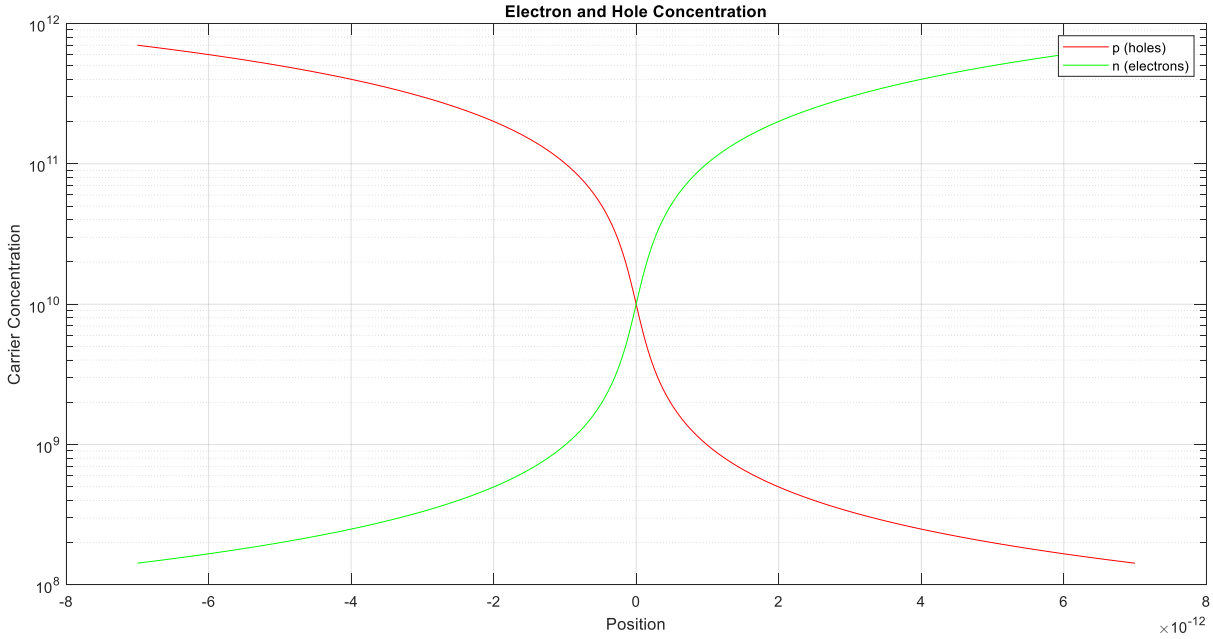
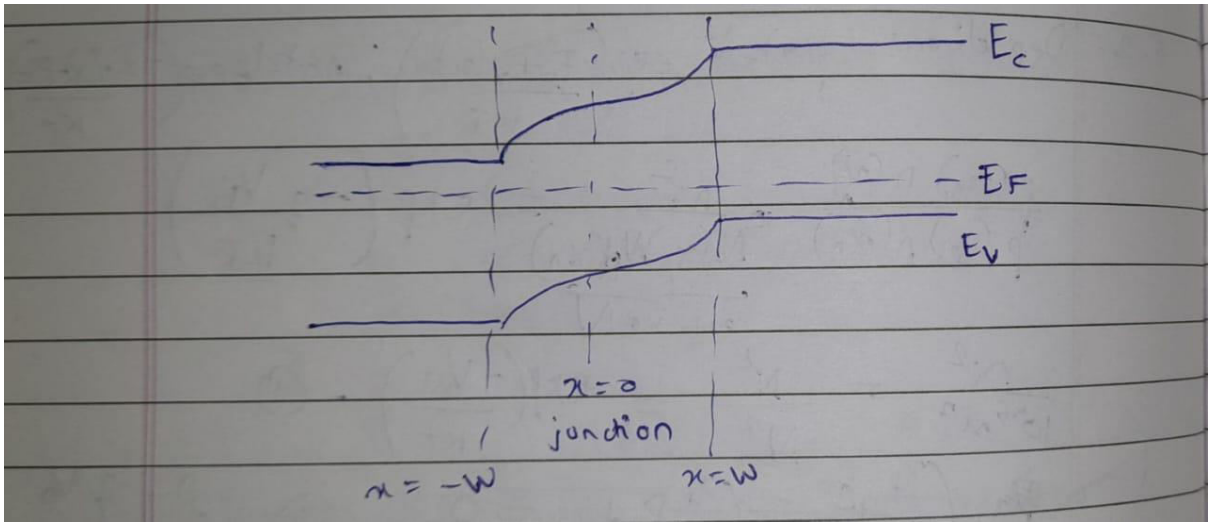
Band Diagram: